NASA Contractor Report 185195

Unified Aeroacoustics Analysis for High Speed Turboprop Aerodynamics and Noise

Volume V - Propagation of Propeller Tone Noise Through a Fuselage Boundary Layer

B. Magliozzi and D. B. Hanson
United Technologies Corporation
Hamilton Standard Division
Windsor Locks, Connecticut

May 1991

Prepared for
Lewis Research Center
Under Contract Number NAS3-23720

National Aeronautics and
Space Administration

NASA Contractor Report 185195

Unified Aeroacoustics Analysis for High Speed Turboprop Aerodynamics and Noise

Volume V - Propagation of Propeller Tone Noise Through a Fuselage Boundary Layer

B. Magliozzi and D. B. Hanson
United Technologies Corporation
Hamilton Standard Division
Windsor Locks, Connecticut

May 1991

Prepared for
Lewis Research Center
Under Contract Number NAS3-23720

National Aeronautics and
Space Administration

CONTENTS

	Page
SUMMARY	1
INTRODUCTION	3
THEORETICAL METHOD DEVELOPMENT	4
Approach	4
Computation of the Wave Field Outside the Boundary Layer	5
Computation of the Wave Field Inside the Boundary Layer	8
Matching of Equations at the Boundary Layer Edge	10
Amplification Plots	10
THEORY VERIFICATION	11
THEORETICAL TRENDS	12
Parameter Dependence	12
Fuselage Scattering Effects	12
Effect of Boundary Layer Profile	12
Effect of Flight Speed	13
Frequency Effects	14
Effect of Scale	15
CORRELATION WITH MODEL PROP-FAN DATA IN FLIGHT	16
Available Data	16
Correlations Using Boom and Fuselage Data	16
Correlations Using Free-Field Calculations	17
CORRECTION FACTORS FOR THE JETSTAR MEASUREMENTS	19
CONCLUDING REMARKS	20
RECOMMENDATIONS	21
REFERENCES	22
APPENDIX A - JETSTAR FUSELAGE MICROPHONE CORRECTION FACTORS	44
APPENDIX B - COMPUTER PROGRAM USER'S GUIDE	55
APPENDIX C - LIST OF SYMBOLS	66

SUMMARY

An analysis of tone noise propagating through a boundary layer and fuselage scattering effects has been derived. This analysis is three-dimensional and the complete wave field is solved by matching analytical expressions for the incident and scattered waves in the outer flow to a numerical solution in the boundary layer flow.

The outer wave field is constructed analytically from an incident wave appropriate to the source and a scattered wave in the standard Hankel function form. For the incident wave, an existing frequency - domain propeller noise radiation theory is used. In the boundary layer region, the wave equation is solved by numerical methods. Over most of the range of axial wavenumber (2π times reciprocal of wavelength in axial direction) this is done using standard numerical integration methods. For large positive wavenumbers, the wave equation acquires a singularity. A Frobenius series expansion is used to represent the solution in the vicinity of the singular point.

The theoretical analysis is embodied in a computer program which allows the calculation of correction factors for the fuselage scattering and boundary layer refraction effects. This analysis allows the use of a boundary layer which is assumed uniform along the fuselage but otherwise arbitrary. The effects are dependent on boundary layer profile, flight speed, and frequency. Corrections can be derived for any point on the fuselage, including those on the opposite side from the source.

The theory was verified using limiting cases and by comparing calculations with available measurements from JetStar tests of model Prop-Fans. In the limiting cases, the large wavelength behavior was verified by calculating the effects for a very small diameter fuselage having a negligible boundary layer. The amplification was calculated to be less than 0.05 dB, indicating that a fuselage this small has negligible effect on the source field. For the small wavelength behavior, a fuselage diameter of 3.05 m (10 ft) was used, again with a negligible boundary layer. This showed an amplification of 6.0 dB, which is the same as the pressure doubling on an infinite plane.

For the JetStar model scale, the boundary layer refraction effects produce moderate fuselage pressure reinforcements aft of and near the plane of rotation and significant attenuation forward of the plane of rotation at high flight speeds. At lower flight speeds, the calculated boundary layer effects result in moderate amplification over the fuselage area of interest. Apparent amplification forward of the plane of rotation is a result of effective changes in the source directivity due to boundary layer refraction effects.

Full scale effects are calculated to be moderate, providing fuselage pressure amplification of about 5dB at the peak noise location.

Evaluation using available noise measurements was made under high-speed, high-altitude flight conditions. Model Prop-Fan noise was measured using microphones flush-mounted in the fuselage and a "free-field" microphone boom installed above the Prop-Fan.

Using the fuselage and boom microphone data, the source effects were eliminated by comparing the measured and calculated boom versus fuselage effects. The agreement between measurements and calculations was good at high flight speeds, but poorer at low flight speeds. This was attributed to refraction effects causing an apparent change in the source directivity. Because the source is modeled as a single monopole, it exhibits a sharp directivity. It is conjectured that a better source representation, including chordwise and spanwise distribution, would "soften" the directivity and improve the agreement with test results.

Comparisons of calculations made of free-field noise, using a current frequency-domain propeller noise prediction method, and fuselage effects using this new procedure show good agreement with fuselage measurements over a wide range of flight speeds and frequencies.

Correction factors for the JetStar measurements made on the fuselage are provided in an Appendix.

INTRODUCTION

The advanced turboprop (Prop-Fan) has been in technology development since 1976 as a fuel-efficient propulsor for the 1990's. As part of the development program, a free-field noise theory[1] based on the acoustic analogy was developed and found to agree well with 1977 test results from an open jet wind tunnel.[2] In 1981, a Prop-Fan model was installed on a business aircraft as shown in Figure 1 for flight noise tests. Microphones were mounted flush with the fuselage surface in axial and circumferential arrays as shown in Figure 2. Because of the small wavelength of the sound and the large fuselage diameter, it was expected that the free space sound levels directly beneath the propeller would be roughly doubled by reflection. However, it was found in early tests that free-space theory, with the 6dB correction for pressure doubling, overpredicted measurements by 10dB or more under some conditions.

After investigating several possible explanations for this over-prediction, a simple analysis of the effect of the fuselage boundary layer on incoming acoustic waves[3] was developed that showed a powerful shielding effect at the high flight Mach number (Mx = 0.8) of the test. The early analysis was 2-dimensional and treated plane waves impinging on a boundary layer over a rigid plane surface. Results for both step and linear boundary layer profiles were given. McAninch, whose analysis[4] included the refinements of a near field source and a curved boundary layer profile, also concluded that significant shielding could occur.

Although these earlier analyses indicated that the fuselage boundary layer effects could be significant, these analyses are not considered sufficiently accurate for prediction of the effects and do not allow the existing JetStar data to be reliably corrected to free-space levels.

In order to allow the existing data to be used and to evaluate the boundary layer propagation effects for other configurations, especially those approaching full-scale in size, the original theory[3] was extended. The extensions include the effects of 3-dimensionality; a near-field, distributed, rotating source; and an arbitrary boundary layer profile using the geometry sketched in Figure 3. The fuselage is modeled as an infinitely long, rigid, circular cylinder with a boundary layer whose properties are constant along its length and circumference.

This work culminated in a computer program which can be used to calculate the boundary layer propagation and fuselage scattering effects on propeller and Prop-Fan noise amplitude. These are intended to be used in conjunction with current noise calculation methods, such as the Unified Aero-Acoustics Program (UAAP), which provide free-field noise estimates. Boundary layer propagation and fuselage scattering effects need to be added to free-field noise estimates for comparison with measurements using transducers flush-mounted on airplane fuselages, as for the NASA SR3/JetStar and SR7/Prop-Fan Test Assessment flight test programs.

The work reported in this document was originally funded by NASA-Ames under contract NAS2-11385.

THEORETICAL METHOD DEVELOPMENT

Approach

The problem described above will be solved by dividing the flow field into a boundary layer region and an outer region assumed to be free of shear. Waves in these two regions will be matched at the boundary layer edge. Following methods given by Morse[5], the outer wave field is constructed analytically from an incident wave appropriate to the source and a scattered wave in the standard Hankel function form. For the incident wave, a frequency-domain propeller radiation theory already exists[1] that is ideally suited to this analysis: its analytical form is in terms of the same Fourier components that occur naturally in the scattered wave and boundary layer wave descriptions so that matching the fields is easily accomplished.

In the boundary layer region, the wave equation must be solved by numerical methods because of the shear term. Over most of the axial wavenumber range, this is easily accomplished with standard numerical integration methods. However, for large positive wavenumbers, the wave equation acquires a singular point and special methods are required. Treatment of this singular point for the corresponding incompressible equation has received considerable attention in the past by Tollmien[6], Lin[7], and Wasow[8] in conjunction with boundary layer instability theory. In more recent times Tam and Morris[9] have addressed the full compressible equation in the analysis of radiation from shear layer instability waves and pointed out that a Frobenius series can be used in the vicinity of the singular point. All these investigators concluded that when the problem is imbedded in the complex plane, the singular point must be spanned by passing beneath it. Treatment of the singular point herein is in accord with the above references.

To establish the general form of waves in axisymmetric shear flow, consider the fuselage-centered coordinates in Figure 4, with positive x measured downstream from the propeller plane of rotation. If the undisturbed velocity U is parallel to the x axis and is a function of r only, then the acoustic pressure outside the source region is given by Goldstein's[10] Equation 1.2.2 .

$$\frac{D}{Dt}\left(D^2 p - \frac{1}{c_o^2}\frac{D^2}{Dt}p\right) - 2U'\frac{\partial p'}{\partial x} = 0 \qquad (1)$$

where primes denote $\partial/\partial r$ and the convective derivative is:

$$\frac{D}{Dt} = \frac{\partial}{\partial t} + U\frac{\partial}{\partial x} \qquad (2)$$

It is easily demonstrated that Equation 1 admits elementary solutions in cylindrical coordinates of the form:

$$P(r)\, e^{ik_x x}\, e^{in\phi}\, e^{-i\omega t} \tag{3}$$

Since we are considering sound from a propeller with B blades and angular speed Ω, the frequency of the m^{th} harmonic is given by $\omega = mB\Omega$ and solutions at this frequency can be constructed from linear combinations of Equation 3 in the following general form.

$$P = e^{-imB\Omega t} \sum_{n=-\infty}^{\infty} e^{in\phi} \int_{-\infty}^{\infty} F_n(k_x)\, P(r)\, e^{ik_x x}\, dk_x \tag{4}$$

where the coefficients F_n are to be found.

The equation for the radial part of the solution, P(r),can be found by substituting Equation 3 into Equation 1 with the Laplacian

$$\nabla^2 = \frac{1}{r}\frac{\partial}{\partial r}\left(r\frac{\partial}{\partial r}\right) + \frac{1}{r^2}\frac{\partial^2}{\partial \phi^2} + \frac{\partial^2}{\partial x^2} \tag{5}$$

The result, with $M = U/c_o$ is:

$$(Mk_x-k)\left(P'' + \frac{1}{r}P'\right) - 2k_x M' P' + (Mk_x-k)\left[(Mk_x-k)^2 - \left(k_x^2 + \frac{n^2}{r^2}\right)\right] P = 0 \tag{6}$$

where $k = \omega/c_o$. At this point we change notation and consider pressure to be normalized by $\rho_o c_o^2$. Also, wavenumbers k and k_x and distances are referred to the boundary layer thickness δ.

Computation of the Wave Field Outside the Boundary Layer

In the outer region the Mach number M is constant at the flight speed value M_x so that $M' = 0$ and Equation 6 reduces to:

$$P'' + \frac{1}{r}P' + \left[(M_x k_x - k)^2 - \left(k_x^2 + \frac{n^2}{r^2}\right)\right] P = 0 \tag{7}$$

This is Bessel's equation with solutions $J_n(k_r r)$ and $Y_n(k_r r)$ where the radial wave number is:

$$k_r = \sqrt{(M_x k_x - k)^2 - k_x^2} \tag{8}$$

The combination of J_n and Y_n corresponding to outgoing waves is the Hankel function:

$$H_n^{(1)} = J_n + i\, Y_n \tag{9}$$

Thus, the scattered wave is given by

$$p = e^{-imB\Omega t} \sum_{n=-\infty}^{\infty} e^{in\phi} \int_{-\infty}^{\infty} E\left[C_n(k_x) + iD_n(k_x)\right] H_n^{(1)}(k_r r)\, e^{ik_x x}\, dk_x \tag{10}$$

where the coefficients C_n+iD_n will be determined when the wave fields inside and outside the boundary layer are matched. The constant $E = Br_T^3/\pi$ has been extracted for later convenience.

For the incident wave, a solution in the form of Equation 4 is easily adapted from an earlier paper by Hanson[1]. In Reference 1, formulas were derived for near-field noise of propellers in forward flight. The theory which treats steady monopole, dipole and quadrupole sources convected along helicoidal paths via the acoustic analogy, has been used routinely at Hamilton Standard since 1977 for propeller and Prop-Fan noise predictions. For economy of space, only the formula for monopole (thickness) noise is given here. However, with the information given, the solution for the other sources could be written down immediately.

For an observer translating with the propeller at flight Mach number M_x, the pressure in the m^{th} harmonic of blade passing frequency is given by

$$p_i = -iE\, e^{imB(\phi - \Omega t)} \int_{ROOT}^{TIP} B_D^2 t_b \int_{-\infty}^{\infty} e^{i\phi_s (M_x k_x - k)^2} \Psi_v^*(k_o)\, J_{mB}(k_r r_T z_o) H_{mB}^{(1)}(k_r r_1)\, e^{ik_x x}\, dk_x\, dz_o \tag{11}$$

where

$$k_o = \frac{2 B_D r_T}{M_r} (M_x k_x - k) \tag{12}$$

$$\phi_s = \frac{-2 r_T}{M_r} (M k_x - k) \quad \frac{MCA}{D} \tag{13}$$

and, as in Reference 1, B is the number of blades, B_D is the chord to diameter ratio, t_b is the thickness to chord ratio, and Ψ_v is the chordwise spatial Fourier transform of the airfoil section thickness distribution. ϕ_s is the phase lag due to sweeping a blade section back along the advance helix by an amount MCA. To establish Equation 11 from Reference 1, a change in notation was made: the k of Reference 1 was changed to $-(M_x k_x - k)/k$ in the present notation and k_x is now the wavenumber of the sound field in the flight direction. In Reference 1, k_x was the chordwise source wave number, a role presently filled by k_o.

In Equation 11, the coordinate system is centered in the propeller axis. The observer is located at r_1, ϕ_1, x. But since the matching process is to be applied at the edge of the fuselage boundary layer, the coordinate system for Equation 11 must be shifted from the propeller axis to the fuselage axis as shown in Figure 4. A Bessel function identity suited for this is given in Reference 11:

$$e^{im\phi} H^{(1)}_{mB}(k_r r_1) = \sum_{n=-\infty}^{\infty} H^{(1)}_{MB+n}(k_r r_{CL}) \; J_n(k_r r) \; e^{in\phi} \qquad (14)$$

When substituted into Equation 11, this gives

$$P_i = e^{-imB\Omega t} \sum_{n=-\infty}^{\infty} e^{in\phi} \int_{-\infty}^{\infty} P_{i,n}(r) \, e^{ik_x x} \, dk_x \qquad (15)$$

where the radial dependence is given by:

$$P_{i,n}(r) = E \, (M_x k_x - k)^2 \, J_n(k_r r) \left[G_{mn}(k_x) + i \, Q_{mn} k_x \right] \qquad (16)$$

and

$$G_{mn}(k_x) + i \, Q_{mn}(k_x) = -iH^{(1)}_{mB+n}(k_r r_{CL}) \int_0^1 B_D^2 \, t_b \, e^{i\phi_s} \Psi_v^*(k_o) \, J_{mB}(k_r r_t z_o) \, dz_o \qquad (17)$$

Note in Equation 17, that the integral contains all the source information.

In Equations 15, 16 and 17, the incident pressure field has been decomposed into time, angle, and axial distance Fourier components. This has been done analytically by virtue of working in the frequency domain. In a time domain source description, this 3-fold Fourier decomposition would have to be done numerically.

Computation of the Wave Field Inside the Boundary Layer

Pressure waves in the boundary layer are solutions to Equation 6 subject to the appropriate boundary condition at the fuselage surface. Equation 6 is somewhat simplified here by dropping the P'/r term leaving

$$(Mk_x-k)P'' - 2k_xM'P' + (Mk_x-k)\left[(Mk_x-k)^2 - (k_x^2 + k_y^2)\right]P = 0 \qquad (18)$$

where for n/r we have written:

$$k_y = n/r \qquad (19)$$

where r is the distance from the fuselage center to the middle of the boundary layer. This approximation is based on the fact that the fuselage radius is much larger than the boundary layer thickness. Thus, the boundary layer region will be solved on a plane in Cartesian coordinates and then "wrapped around" the fuselage. Periodicity in ϕ is guaranteed by requiring that n be an integer. This approximation could easily be eliminated but it doesn't seem worthwhile at this point considering that the assumptions of a uniform boundary layer and a circular section fuselage are also approximate in most cases.

To solve Equation 18, we shift the origin of the radial coordinate to the fuselage:

$$r = r_f + z \qquad (20)$$

so that the normal coordinate in the boundary layer is z, which runs from 0 at the fuselage to 1 at the boundary layer edge. Over most of the range of interest in k_x, Equation 18 is integrated by a standard Runge-Kutta method. However, for $k_x > k/M_x$, the factor $Mk_x - k$ goes to zero for some value of z between 0 and 1. This point, z_s, is a singular point of Equation 18 and requires special treatment. The method used here is to apply the Runge-Kutta integration from $z = 0$ to within a few mesh points of z_s where it is matched to a series solution about z_s. The series solution spans the singular point a few mesh points beyond z_s where the Runge-Kutta integration is continued to $z = 1$.

For the series about z_s, we use the method of Frobenius[12] as suggested by Tam and Morris[9]. This is straightforward to apply and yields an indicial equation with roots equal to 0 and 3 so the two linearly independent series solutions are:

$$P_A = (z - z_s)^3 \left[1 + a_1(z - z_s) + a_2(z - z_s)^2 + \ldots\right] \qquad (21)$$

$$P_B = 1 + b_1(z - z_s) + b_2(z - z_s)^2 + \ldots + C\,P_A \ln(z - z_s) \qquad (22)$$

With two series, the numerical result can be matched for P and P'. The coefficients a_n, b_n and C depend on the Mach number profile in the boundary layer and can be found by substitution into Equation 18.

When the series in Equations 21 and 22 are matched to the numerical result on the fuselage side of the singular point ($z < z_s$), a decision must be made regarding branches of the log function. This issue has been discussed extensively in the literature in conjunction with studies of boundary layer instability using the 2D incompressible version of Equation 18. The early work by Tollmien, Lin[7], Wasow[8] is summarized by Schlichting[13] where it is shown that the branch of the logarithm must be taken such that $\ln (z - z_s) = \ln |z - z_s| - i\pi$ for $z < z_s$. This was proved by examination of a more complete fourth order differential equation for the flow that, because it includes viscosity, is not singular at z_s. Tam and Morris[9], in their work on sound from compressible shear layer instability waves, arrived at the same conclusion using different methods. They showed that the singular point may be spanned by embedding the problem in the complex plane and passing beneath z_s.

With respect to the form that waves may take in the vicinity of the critical layer ($z = z_s$), the Tam and Morris[9] analysis and the present analysis are dealing with different aspects of the same physical problem. Hence, we follow their precedent and use $\ln(z - z_s) = \ln |z - z_s| - i\pi$ for $z < z_s$.

For conditions with or without a singular point unit solutions, $P_n(k_x,z)$, to Equation 18 for any k_x and n are obtained by integrating from z = 0 to 1 starting with the boundary conditions:

$$\tilde{P}_n(k_x,0) = 1 \quad ; \quad \tilde{P}'_n(k_x,0) = 0 \tag{23}$$

The general solution in the boundary layer region is then:

$$P_{BL} = e^{-im\beta\Omega t} \sum_{n=-\infty}^{\infty} e^{in\phi} \int_{-\infty}^{\infty} \left[A_n(k_x) + iB_n(k_x)\right]\tilde{P}_n(k_x,z)\, e^{ik_x x}\, dk_x \tag{24}$$

where $A_n(k_x)$ and $B_n(k_x)$ are to be found by matching to the outer field.

Matching of Equations at the Boundary Layer Edge

We now have expressions for the wave field outside the boundary layer, $P_S + P_i$ from Equations 10 and 15, and for the boundary layer wavefield P_{BL} from Equation 24. These have to be matched at the boundary layer edge $r = r_E$ for all x, ϕ, and t. Here the matching is achieved equivalently in the frequency/wavenumber domain for all k_x, n, and m. Thus, the matching equations for pressure and its derivative are:

$$E\left[(M_x k_x - k)^2 J_n(k_r r_E)(G_{mn} + iQ_{mn}) + (C_n + iD_n) H_n^{(1)}(k_r r_E)\right] = (A_n + iB_n)\tilde{P}_n(k_x, 1)$$

$$Ek_r\left[(M_x k_x - k)^2 J_n'(k_r r_E)(G_{mn} + iQ_{mn}) + (C_n + iD_n) H_n'^{(1)}(k_r r_E)\right] = (A_n + iB_n)\tilde{P}_n'(k_x, 1)$$

The real and imaginary parts of these equations yield four equations that can be solved for A_n, B_n, C_n and D_n, giving the entire wave field. In particular, Equation 24 gives the pressure on the fuselage surface ($z = 0$) with $\tilde{P}_n(k_x, 0) = 1$.

Amplification Plots

The theory derived above provides means of predicting the absolute amplitude and phase of propeller noise on a fuselage surface with a boundary layer. However, since the purposes of this study are to investigate the effects of the fuselage and boundary layer and to provide corrections to free-space levels, most results are presented as amplifications. Thus, 6dB would represent the usual doubling effect of a hard wall; lower amplifications indicate boundary layer shielding or fuselage shadowing.

Amplification is defined as the ratio in dB between the acoustic pressure with fuselage and boundary layer, to the acoustic pressure at the same location in space but without the fuselage and boundary layer. Thus,

$$\text{Amplification} = 20 \log_{10}\left[\frac{(P_{BL})_{RMS}}{(P_i)_{RMS}}\right] \quad \text{dB} \qquad (27)$$

where both pressures are computed at $r = r_f$ and are functions of x and ϕ. In order to study fuselage effects without confusion due to chordwise and spanwise interference within the propeller source, the blades were replaced by point sources at 80% of the blade radius. The chordwise thickness distribution is compressed to a point by using the chordwise transform for zero chord:

$$\Psi(k_0) = \Psi(0) \qquad (28)$$

A plot of amplification as a function of x and ϕ for conditions typical of the JetStar/Prop Fan model flight tests is shown in Figure 5 . Behind the plane of rotation, the combination of boundary layer attenuation and finite fuselage diameter results in an amplification of about 4dB (slightly less than the 6dB expected for full pressure doubling). At the forward location, significant attenuation appears due to the boundary layer refraction effects. Transverse to the airplane axis it can be seen in Figure 5 that the peak amplification occurs at about -10 degrees. This is a function of the direction of rotation of the Prop-Fan and is due to the source directivity. As would be expected, the amplification falls off on either side of the centerline because of grazing incidence.

THEORY VERIFICATION

Although the amplification curves presented above exhibit the general behavior expected from previous experience with respect to shielding and shadowing effects, the theory was verified further in the numerical experiment described below.

First the scattering theory was checked by running some limiting cases with an infinitesimally thin boundary layer. The large wavelength behavior of the theory was verified by running a JetStar case with the fuselage diameter reduced to 0.03 mm (0.0001 ft). The resulting amplification was less than .05 dB, indicating that a fuselage this small has negligible effect on the source field. In order to check the small wavelength behavior of the theory, a fuselage diameter of 3.05 m (10 ft) was used. This produced an amplification of 6.0 dB. This is the same as the pressure doubling on an infinite plane, again verifying correct behavior. To check behavior at intermediate wavelength, comparisons were made with published curves for plane waves impinging on cylinders with no flow.[14] When plane waves were simulated by moving the source far from the fuselage, the predicted surface pressures matched those of Reference 14.

Propagation within the boundary layer was checked by reproducing McAninch's 2D amplitude results[4] for individual frequencies and wavenumbers. This was done by integrating Equation 18 with $k_y = 0$. The comparison with McAninch is shown in Figure 6 for a typical case. The curves represent amplification according to

$$\Delta dB = 20 \log_{10}\left[\frac{(P_{BL})_{RMS}}{(P_E)_{RMS}}\right] \tag{29}$$

where P_{BL} is pressure on the surface under the boundary layer and P_E is the pressure in the incident wave measured at the boundary layer edge.

As a final check of the theory, the equivalence of Equation 11 and Equations 15-17 was verified. These are source noise formulas expressed in source coordinates and in fuselage coordinates respectively. Although the expression in fuselage coordinates is considerable more complicated, values for the free space levels calculated using Equations 15-17 typically agree within less than 0.1 dB with those calculated using Equation 11.

THEORETICAL TRENDS

Parameter Dependence

The present theory allows the calculation of fuselage scattering and boundary layer refraction effects. These effects depend on many parameters such as: boundary layer profile, boundary layer thickness, flight speed, frequency, fuselage diameter, and incidence angle. Currently, the analysis is configured to provide amplitude correction factors between free-space sound pressure levels and those at the fuselage surface. In the implementation of the calculation procedure, fuselage locations are specified relative to the Prop-Fan plane-of-rotation. Also, because the present theory includes fuselage scattering effects, it is possible to predict the variation of noise circumferentially around the fuselage.

Fuselage Scattering Effects

Figure 7 shows the calculated correction factor as a function of angle around a fuselage. This calculation was done assuming a negligible boundary layer for a flight Mach number of 0.8. Although the geometry used for this example is that of a Prop-Fan model test, it illustrates the scattering effects. Comparable results would be expected in full-scale. As can be seen, the calculated effects are similar for the three axial positions. Near 0 degrees, the fuselage produces full pressure doubling. At positions around the fuselage, the pressure reinforcing effects decrease and beyond about 50 degrees a shadow zone begins. On the opposite side of the fuselage, near 180 degrees, a strong shadow zone may be seen. As expected, the shadow zone is stronger for 3XBPF than for BPF, as the wavelength is shorter for the higher frequency. Also, the 6dB plateau is wider for the higher harmonic. Finally, it may be noted that the pattern is not centered on 0 degrees, but appears shifted by about 15 degrees. This is a result of the Prop-Fan direction of rotation, as was also seen in Figure 5.

In general, the scattering effects show some degree of pressure reinforcement near the point of closest approach of the Prop-Fan and a shadow zone on the far-side of the fuselage. The amount of pressure reinforcement is dependent on the size of the fuselage relative to the wavelength of the incoming sound waves, as is the depth of the shadow zone. Figure 7 shows typical results. It was previously shown that a very small fuselage gave essentially no scattering effects, while a large fuselage produced full pressure doubling.

Effect of Boundary Layer Profile

The amount of boundary layer refraction effect is dependent on the shape of the velocity profile within the boundary layer. To evaluate this dependence, calculations were done for representative configurations using several boundary layer profiles. For this study, four profiles were evaluated. The profiles are shown in Figure 8 in JetStar scale. The linear profile is the simplest and has no higher derivatives within the boundary layer. The slope, M', in Equation 18 is constant. The 1/7 power law curve is representative of a classic turbulent boundary layer. The 1/3 power law was used to illustrate the dependence of the velocity gradient within the boundary layer. The

1/3 power law profile also effectively results in a thicker boundary layer. These three profiles are used with a boundary layer thickness of 0.13 m (0.42 ft), which is approximately what would be expected on a flat plate. Also, the boundary layer measurements made on the JetStar, shown in Figure 9, show this to be a reasonable boundary layer thickness. It should be noted, however, in Figure 9 that the velocity reached at about 0.14 m (0.46 ft) is only 96% of the edge velocity. The flow velocity then decreases followed by a second reversal in slope. For these measurements, the edge velocity was measured at the Prop-Fan centerline. Although this would place the boundary layer edge at the Prop-Fan center, the present boundary layer analysis is based on the source being totally outside of the boundary layer. Thus, for these evaluations, the boundary layer edge was assumed to be just beyond the Prop-Fan blade tips, at 0.48 m (1.58 ft) from the fuselage surface. The boundary layer profile labeled "JetStar" in Figure 8 is thus based on a linear interpolation of the JetStar measurements to 0.20 m (0.67 ft), then extrapolated to an edge assumed to be 0.48 m (1.58 ft) from the fuselage. As may be noted in Figure 8 the JetStar profile is very simular to the classic 1/7 power law profile to about 0.08 m (0.25 ft) from the surface. Beyond 0.13 m (0.42 ft) the "JetStar" profile has only gentle gradients and would not be expected to give results much different from the 0.13 m (0.42 ft) thick boundary layers.

Figure 10 shows the calculated boundary layer effects on model Prop-Fan noise based on the four profiles described in Figure 8. As may be seen, the linear boundary layer profile has the greatest effect, showing significant attenuation over the entire range of axial positions. The JetStar and 1/7 power law profiles show generally similar results, with the JetStar having slightly more effect from 0.46 m (1.5 ft) aft to 0.30 m (1 ft) forward of the plane of rotation. From about 0.15 m (0.5 ft) forward of the plane of rotation aft the 1/7 power law boundary layer profile results in a correction of 3 to 4 dB, representing pressure reinforcement caused by the fuselage. The 1/3 power law boundary layer profile shows effects between those for the 1/7 power law profile and the linear profile, as would be expected as the effective boundary layer thickness is between those. All four profiles show significant refraction effects forward of the plane of rotation.

It is apparent that the boundary layer profile has a significant effect on the propagation effects. The measured JetStar boundary layer profile is similar to the classic 1/7 power law profile for turbulent boundary layers. The propagation effects for the JetStar boundary layer are also similar to those for the 1/7 power law profile. Calculations using the measured JetStar boundary layer will be used in subsequent discussion.

Effect of Flight Speed

The boundary layer refraction and fuselage scattering effects depend on flight Mach number. The Mach number dependence is illustrated in Figure 11, which shows the calculated corrections along the $\Phi = 0$ line on the JetStar fuselage for the BPF of the SR2 Prop-Fan operating at $M_T = 0.8$. At 0.8 Mach number, a modest pressure reinforcement appears aft of the plane of rotation. Forward of the plane of rotation, appreciable attenuation may be seen. The attenuation is caused by refraction effects in the boundary layer. At 0.7 and 0.6 Mach numbers, pressure reinforcement also appears aft of the plane of

rotation. The effect initially decreases in the forward direction, but then appears to increase again. The 0.7 Mach number curve appears to peak at about 0.46 m (1.5 ft.) forward of the plane of rotation, then shows a decrease. The 0.6 Mach number curve is still rising beyond the range calculated. At 0.61 m (2 ft.) forward, the apparent fuselage effect is 9dB. This is greater than would be expected from a pressure amplification effect. A possible explanation for this is that the propagation through the boundary layer results in an apparent change in source directivity, as illustrated in Figure 12. In the absence of any boundary layer, the acoustic ray would travel to the receiver following the direct path. For the effective radius source represented, the directivity angle is indicated as θ. With the boundary layer present, the acoustic ray is refracted and follows the path labeled "refracted path". As shown, the refracted ray is at a directivity angle θ_R, which is closer to the plane of rotation than the angle θ. The source characteristics are such that the noise peaks near the visual plane of rotation, so that there is significantly more noise along θ_R than along θ. The receiver then observes more noise due to the apparent directivity change caused by the refraction effects. At higher flight speeds, or at further forward positions, refraction is complete and the sound is greatly attenuated before reaching the receiver. Apparently, for the 0.7 Mach number curve in Figure 11, the peak at 0.46 m (1.5 ft.) forward is due to the directivity change caused by the boundary layer refraction effects. The correction then decreases again, as refraction becomes more complete.

Figure 13 shows the calculated effects of flight speed on the 3XBPF harmonic. Similar effects to those for the BPF harmonic are seen to occur. However, due to the smaller source wavelength the effects are more pronounced. At 0.8 Mx there appears a strong attenuation effect. At 0.7 Mx, there appears a modest reinforcement, again due to refraction effects on the apparent source directively, then a strong attenuation effect as refraction becomes more complete. At 0.6 Mx, the directivity effects are even stronger than for the BPF tone, which is expected since the source directivity becomes sharper with increasing frequency.

Frequency Effects

The calculated fuselage boundary layer effects are shown in Figure 14 as a function of frequency. For this illustration, the effects were calculated for a flight Mach number of 0.7. The effects of frequency are seen in the three harmonics of blade passing frequency calculated. At low frequency, the behavior is as previously discussed. At 2XBPF, the peak has moved aft, consistent with a sharper source directivity. It can be seen that beyond 0.46 m (1.5 ft.), the exponential decay effect has occurred, as full refraction through the boundary layer is occurring. At 3XBPF, the peak is still further aft, consistent with the still-sharper directivity at this higher frequency.

It is thus apparent that the fuselage boundary layer refraction effects are strongly dependent on frequency. This should not be surprizing, as the source wavelength to boundary layer thickness ratio decreases with increasing frequency thereby producing more refraction effects within the boundary layer.

Effect of Scale

The above discussion is in the context of the JetStar model Prop-Fan scale. For the JetStar cases, a relatively thick boundary layer, based on measurements, has been used in the calculations. Further, the small size of the Prop-Fan models resulted in relatively short wavelengths for the source. It was found that for these small size configurations, the pressure reinforcement near the peak noise directivity at 0.8 flight Mach number is in the order of 2 to 3 dB. This is less than the usual 6 dB pressure doubling assumed for typical fuselage effects. However, the effect was found to be frequency dependent, so that these results might not be as strong in full-scale.

The boundary layer/fuselage effects for a full-scale Prop-Fan configuration were calculated for an 8-bladed, 4.57 m (15.0 ft.) diameter Prop-Fan operating at 0.8 Mach number cruise and a tip clearance of 0.8 diameter. The fuselage was assumed to be 3.66 m (12.0 ft) in diameter with a 0.10 m (0.33 ft) thick boundary layer. The boundary layer used is a classical one with a 1/7 power law profile.

Figure 15 shows the calculated effects for the first two harmonics of blade passing frequency. From aft of the plane of rotation to slightly forward of the plane of rotation the fuselage correction is between 5 and 6 dB. The BPF tone shows a very slight boundary layer refraction effect forward of the plane of rotation. The refraction effects are stronger for the 2XBPF tone and substantial attenuation becomes apparent beyond about 0.5 diameters. However, the free-field noise of Prop-Fans tends to peak near the visual plane of rotation. From Figure 15 it can be seen that in the plane of rotation the correction is 5 dB for both the BPF and 2XBPF tones. Thus, it would appear that the fuselage/boundary layer effects for a full scale Prop-Fan installation operating at high Mach number cruise would be only about 1 dB less than full pressure doubling.

CORRELATION WITH MODEL PROP-FAN DATA IN FLIGHT

Available Data

The available model data includes noise measurements made under actual high-speed, high altitude flight conditions. Model Prop-Fan noise was measured using microphones flush-mounted in the fuselage. Also, a limited number of test flights were made with a "free-field" microphone boom installed above the Prop-Fan. The microphone installations are shown in Figure 16. Acoustic results from this series of tests were reported in References 15 and 16.

Correlations Using Boom and Fuselage Data

The boom contained four microphones, installed at axial locations and radial tip clearances corresponding to four microphone locations on the JetStar fuselage. Because of its thin boundary layer and small diameter (0.038 m (0.125 ft)), it was expected that the boom noise levels would be representative of levels in free space and would therefore be useful for direct comparison with the fuselage levels. This turned out not to be the case, as the convection effect reduces the wavelength of noise at blade passing frequency to approximately 0.10 m (0.33 ft), and significant scattering occurs at the boom. However, the present theory can be used to evaluate these effects by comparing the calculated noise at the boom and at the fuselage and then comparing that result with the corresponding measurements. This is readily seen from the relationship:

$$SPL_B - SPL_{FS} = \Delta SPL_B \qquad (30)$$

$$SPL_F - SPL_{FS} = \Delta SPL_F \qquad (31)$$

where SPL_B is the sound pressure level at the boom microhone location, SPL_{FS} is the free-space sound pressure level and SPL_F is the sound pressure level at the fuselage microphone locations. Since the boom was located at the same distance from the Prop-Fan center as the fuselage,

corresponding microphone locations have the same free-space sound pressure level. By equating SPL_{FS} in equations 30 and 31, we obtain $SPL_B - SPL_F = \Delta SPL_B - \Delta SPL_F$. Thus, the measured SPL at the boom minus the measured SPL at the fuselage is equal to the difference between the boom effects and the fuselage effects. Since the latter is calculated by the present theory, a comparison can be made to evaluate the calculations. This approach has the advantage of not requiring that the Prop-Fan source characteristics be known. Table I shows comparisons for several representative conditions.

The two high flight Mach number conditions, at 0.787, show generally good agreement. The trend showing that the fuselage boundary layer effects are stronger for the forward microphone locations is seen in both the measurements and the calculations. At lower flight speeds, the agreement between the measurements and the calculations deteriorates. In general, the measurements show consistent fuselage boundary layer effects which provide attenuation.

The calculations generally show some degree of amplification. The apparent amplification effects were previously described and identified as an apparent source directivity change caused by boundary layer refraction effects (see Figure 12). This apparent amplification is not supported by the data. However, it should be recalled that for the present analysis the source representation is chordwise and spanwise compact. In actuality, the Prop-Fan noise source is distributed, so that the refraction effects are different for each source element. Integrating the effect over the blade span thus "softens" the effect. In addition, a complete source representation, including loading noise dipoles and quadrupoles, would also reduce the apparent amplification effects by broadening the source directivity.

It may be noted that the data show some of these effects, albeit not to the same degree as presently calculated. For example, the 0.620 Mx case for the SR3 model shows a peak value of 131.3 dB at the BPF measured on the boom. At the forward microphone, the level has dropped to 124.6 dB, a change in directivity of 6.7 dB. The corresponding fuselage microphones show a difference of 6.6 dB, or almost the same. However, at 3XBPF the difference from peak to the forward location sound pressure level is 11.7 dB at the boom, but only 7.2 dB at the fuselage. This appears to indicate that the fuselage boundary layer effects have broadened the directivity pattern on the fuselage.

As a final note, it is assumed in this comparison that the boom is isolated. In actuality, there will be reflections from the fuselage which will affect the boom data. These effects cannot be calculated using the current method, as it is restricted to having the observer on the fuselage. However the theory allows the observer to be located at any lpoint in space and the method can be generalized with some further work.

Correlations Using Free-Field Calculations

Another way to evaluate the fuselage effects theory is to calculate free-field sound pressure levels, apply the fuselage correction, and then compare these with the measurements. Figure 17 shows comparisons between measured and calculated JetStar fuselage microphone data for the SR3 Prop-Fan model operating at a flight speed of 0.787 Mn. The free-field source levels were calculated using Hanson's frequency domain method[1] and the fuselage corrections were calculated using the present analysis. The boundary layer propagation effects result in substantial attenuation at the forward microphone locations. At the rearward microphones, the fuselage pressure amplification effects are about 1 to 2 dB. The boundary layer attenuation effects increase with increasing frequency. These predictions are borne out by the measurements.

Figure 18 shows similar comparisons at a flight speed of 0.713 Mn. For this lower flight speed, the boundary layer effects show an increase over free-field levels at all measurement locations. At the aft locations, the increase is modest (up to about 4 dB) and is due to pressure amplification caused by the fuselage. At the forward locations, the effect of the boundary layer is greater, reaching more than 9 dB at 3XBPF. This appears to be a combination of fuselage reflection and a bending forward of the source directivity pattern by refraction in the boundary layer. This effect is slightly

over-calculated at BPF, but agrees well with measurements at 2XBPF and 3XBPF. Certainly the free-field predictions are improved by the corrections calculated using the present theory, especially at the forward locations.

Figure 19 shows a comparison at a still lower flight speed. Again, the boundary layer effects for this 0.620 flight Mach number case show amplification at the forward microphone locations. Except for the most forward microphone at BPF, the agreement between the calculations and the measurements in much improved by the boundary layer propagation effects corrections.

It is apparent from the comparisons presented in Figures 17, 18 and 19 that the boundary layer propagation effects corrections calculated using the present theory significantly improve the predictions. Noise predictions made using the Hanson frequency domain analysis[1] and fuselage scattering/boundary layer propagation effects calculated using the current method show good agreement with measurements made on the JetStar fuselage.

CORRECTION FACTORS FOR THE JETSTAR MEASUREMENTS

Using the present theory, boundary layer propagation/fuselage scattering effects corrections have been calculated for the JetStar test conditions. Since the available test data span a wide range of operating conditions, the calculations were done for a matrix of operating conditions which bracket the test data. A complete set of correction factors is given in Appendix A.

For these correction factors, calculations were made for all combinations of flight speeds of 0.6, 0.7, and 0.8 Mn, and 1, 2, and 3 times blade passing frequency for an 8-bladed Prop-Fan. These allow corrections for the available data to be derived by interpolation. The corrections are applicable to both SR2 and SR3 in their 8-bladed test configurations. It should be noted that the corrections given are defined as fuselage levels minus free-field levels. Thus, subtracting the correction given in Appendix A from the sound pressure level measured by the fuselage microphones will result in levels corrected to free-field conditions. Conversely, adding the correction to calculated free-field levels gives the estimated level on the fuselage.

The corrections given are independent of altitude and Prop-Fan power loading.

CONCLUDING REMARKS

In this report a new theoretical analysis has been presented that solves the entire acoustic field around a cylindrical fuselage with a boundary layer in the presence of incident waves from a distributed propeller noise source. Scattering from the boundary layer, reflection from the fuselage, and refraction in the boundary layer are all rigorously accounted for. The theory represents the propeller with multiple blades and sources distributed over their chords and spans. However, to derive general correction curves for this report as functions of gross operating conditions, the source representation was simplified to a single point thickness source for each blade. This eliminates any chordwise and spanwise interference that would be peculiar to a particular blade design. Correction curves have been presented that represent the difference between noise levels predicted on the fuselage surface and the levels predicted at the same point in space but without the fuselage and boundary layer.

Based on studies of these correction curves, the following conclusion have been reached.

1. In general, the theory predicts attenuation forward of the plane of rotation and modest amplification aft of the plane of rotation for the SR2 and SR3 model Prop-Fans on the JetStar at high cruise Mach numbers.

2. At low flight speeds, the theory predicts amplification at all locations for the SR2 and SR3 model Prop-Fans. This appears to be a result of the apparent change in source directivity caused by boundary layer refraction.

3. The theory indicates for a full scale Prop-Fan that the fuselage scattering/boundary layer refraction effects result in a pressure amplification of approximately 5 dB at the peak noise location. This amplification reduces to 2.5 dB at the blade passing frequency and to a reduction of 2.5 dB at 2 times blade passing frequency at 0.8 diameters forward of the plane of rotation.

4. The calculated fuselage scattering/boundary layers refraction effects show a strong dependence on frequency.

5. Comparison between theory and JetStar test data is generally good when predictions are made by using the existing Hamilton Standard free-space Prop-Fan noise prediction procedure with corrections from the new boundary layer propagation analysis.

6. Comparisons are not as good when using the boundary layer propogation theory to predict the differences between JetStar fuselage surface levels and JetStar microphone boom levels. It is not known at this point whether this is a problem with the theory or with the boom data.

RECOMMENDATIONS

In this report the new theory has been demonstrated to provide improved accuracy on the basis of amplitude when used to correct free space predictions to fuselage levels. Both amplitude and phase information are needed for fuselage treatment design. Therefore its phase accuracy should also be evaluated. Also, the disagreement with the microphone boom results should be investigated. This disagreement must be understood to establish the value of a "free-space" boom in future flight tests.

REFERENCES

1. Hanson, D.B., "Near-Field Frequency-Domain Theory for Propeller Noise," AIAA Paper No. 83-0688 (to be published by AIAA Journal).

2. Brooks, B. and Metzger, F. B., "Acoustic Test and Analysis of Three Advanced Turboprop Models," NASA CR-159667, Jan. 1980.

3. Hanson, D.B., "Shielding of Prop-Fan Cabin Noise by the Fuselage Boundary Layer," Hamilton Standard Engineering Report, HSER 8165, August 24, 1981. (Also to appear in Journal of Sound and Vibration on March 8, 1984).

4. McAninch, G.L., "A Note on Propagation through a Realistic Shear Layer," Letter to the Editor in Journal of Sound and Vibration, Vol. 88, No. 2, pp. 271-274, 1983.

5. Morse, P.M., Vibration and Sound, McGraw-Hill, New York, 1948.

6. Tollmien, W., "The Production of Turbulence," NACA TM609, Washington, D.C., 1931.

7. Lin, C. C., "On the Stability of Two-Dimensional Parallel Flows," Quarterly of Applied Mathematics, Vol. 3, pp. 117-142 (Part I) and pp. 218-234 (Part II), 1945.

8. Wasow, W., "The Complex Assymptotic Theory of a Fourth Order Differential Equation of Hydromechanics," Annals of Mathematics, Vol. 49, No. 4, October 1948.

9. Tam, C.K.W and Morris, P.J., "The Radiation of Sound by the Instability Waves of a Compressible Plane Turbulent Shear Layer," J. Fluid Mechanics, Vol. 98, Part 2, pp. 349-381, 1980.

10. Goldstein, M.E., Aeroacoustics, McGraw-Hill, New York, 1976.

11. Abramowitz, M. and Stegun, I.A. (Editors), Handbook of Mathematical Functions, National Bureau of Standards, Washington, D.C., 1964.

12. Korn, G.A. and Korn, T.M., Mathematical Handbook for Scientists and Engineers, McGraw-Hill, pp. 257-260, 1968.

13. Schlichting, H., Boundary Layer Theory (Seventh Ed.), McGraw-Hill, New York, pp. 438-450, 1979.

14. Wiener, F.M., "Sound Diffraction by Rigid Spheres and Circular Cylinders," J. Acoustical Society of America, Vol. 19, No. 3, May 1947, pp. 444-451.

15. Brooks, B.M., Analysis of Jetstar Prop-Fan Acoustic Flight Test Data, Hamilton Standard HSER 8882, November 1983.

16. Hamilton Standard, JetStar Propeller Flight Test Program Acoustic Data Report, Prepared under contract NAS4-2822, May 1982.

TABLE I - Comparison of Measured and Calculated Fuselage Effects for the JetStar Test Airplane

Prop-Fan Configuration	Flight Mn	Harmonic	Mic No. Boom/Fuse	Measured SPL Boom	Measured SPL Fuse	Calculated ΔSPL Boom	Calculated ΔSPL Fuse	ΔdB, Boom-Fuse Meas.	ΔdB, Boom-Fuse Calc.
SR3	0.787	1	1/3	133.1	127.0	2.3	-1.7	6.1	4.0
			2/4	-	136.0	2.8	0.5	-	2.3
			3/5	143.0	140.4	3.2	0.8	2.6	2.4
			4/7	146.1	141.3	3.2	1.3	4.8	1.9
		2	1/3	129.8	110.4	2.6	-14.9	19.4	17.5
			2/4	-	129.1	3.3	-2.4	-	5.7
			3/5	138.4	136.5	3.8	0.6	1.9	3.2
			4/7	137.9	136.3	4.2	0.5	1.6	3.7
		3	1/3	126.3	105.8	2.1	-21.9	20.5	23.0
			2/4	-	120.5	3.3	-5.2	-	8.5
			3/5	133.8	129.3	4.2	1.3	4.5	2.9
			4/7	135.8	118.6	4.6	0.3	17.2	4.3
	0.713	1	1/3	130.0	127.2	1.6	4.8	2.8	-3.2
			2/4	-	132.1	2.1	3.2	-	-1.1
			3/5	139.3	136.2	2.4	1.9	3.1	0.5
			4/7	140.2	134.0	2.4	2.0	6.2	0.4
		2	1/3	126.7	121.1	3.8	7.3	5.6	-3.5
			2/4	-	129.6	3.9	4.6	-	-0.7
			3/5	137.2	133.6	4.1	2.1	3.6	2.0
			4/7	136.9	130.9	4.4	1.0	6.0	3.4
		3	1/3	122.7	116.4	4.0	8.7	6.3	-4.7
			2/4	-	126.2	4.1	6.0	-	-1.9
			3/5	132.6	128.6	4.1	2.3	4.0	1.8
			4/7	129.6	120.0	4.2	0.3	9.6	3.9
	0.620	1	1/3	124.6	119.8	1.1	5.5	4.8	-4.4
			2/4	-	123.0	1.4	3.8	-	-2.4
			3/5	131.3	126.4	1.6	2.7	4.9	-1.1
			4/7	122.6	125.5	1.5	2.2	-2.9	-0.7
		2	1/3	113.8	112.7	3.8	8.9	1.1	-5.1
			2/4	-	115.2	3.9	5.5	-	-1.6
			3/5	120.3	116.9	4.0	3.1	3.4	0.9
			4/7	122.7	118.0	4.2	1.9	4.7	2.3
		3	1/3	107.6	106.4	4.4	12.1	1.2	-7.7
			2/4	-	111.5	4.2	6.8	-	-2.6
			3/5	113.4	107.9	4.2	3.1	5.5	1.1
			4/7	119.3	113.6	4.3	1.2	5.7	3.1

TABLE I - Comparison of Measured and Calculated Fuselage Effects for the JetStar Test Airplane (Continued)

Prop-Fan Configuration	Flight Mn	Har-monic	Mic No. Boom/Fuse	Measured SPL Boom	Measured SPL Fuse	Calculated ΔSPL Boom	Calculated ΔSPL Fuse	ΔdB, Boom-Fuse Meas.	ΔdB, Boom-Fuse Calc.
SR2	0.787	1	1/3	139.6	-	2.0	-1.3	-	3.3
			2/4	148.2	146.5	2.6	0.4	1.7	2.2
			3/5	151.0	149.0	3.1	0.6	2.0	2.5
			4/7	151.0	144.0	3.1	1.2	7.0	1.9
		2	1/3	136.2	-	2.8	-9.1	-	11.9
			2/4	142.5	140.0	3.4	-0.7	2.5	4.1
			3/5	145.6	137.9	3.9	0.4	7.7	3.5
			4/7	134.0	136.3	4.3	0.2	-2.3	4.1
		3	1/3	131.5	-	2.5	-17.9	-	-
			2/4	139.0	135.2	3.5	-2.0	3.8	5.5
			3/5	142.8	130.6	4.2	1.0	12.2	3.2
			4/7	133.9	112.6	4.5	-0.5	21.3	5.0
	0.710	1	1/3	139.0	137.8	1.6	4.6	1.2	-3.0
			2/4	145.6	142.0	2.1	3.0	3.6	-0.9
			3/5	145.0	142.5	2.3	1.9	2.5	0.4
			4/7	142.0	136.7	2.2	1.7	5.3	0.5
		2	1/3	131.6	128.9	3.8	7.4	2.7	-3.6
			2/4	137.6	135.0	4.0	4.3	2.6	-0.3
			3/5	138.8	139.6	4.1	1.8	-0.8	2.3
			4/7	141.1	125.8	4.5	1.1	15.3	3.4
		3	1/3	128.6	126.3	4.1	9.3	2.3	-5.2
			2/4	136.2	133.1	4.1	5.6	3.1	-1.5
			3/5	136.1	132.9	4.1	1.9	3.2	2.3
			4/7	130.9	121.4	4.2	0.2	9.5	4.0
	0.617	1	1/3	124.0	119.7	0.9	5.6	4.3	-4.7
			2/4	128.2	123.5	1.2	3.9	4.7	-2.7
			3/5	129.3	127.2	1.4	2.8	2.1	-1.4
			4/7	125.3	123.0	1.3	3.0	2.3	-1.7
		2	1/3	114.8	104.1	3.6	8.5	10.7	-4.9
			2/4	121.9	109.4	3.7	5.1	12.5	-1.4
			3/5	119.9	112.9	3.8	2.8	7.0	1.0
			4/7	115.3	113.4	4.0	2.0	1.9	2.0
		3	1/3	107.1	100.7	4.4	11.3	6.4	-6.9
			2/4	112.7	103.9	4.2	6.2	8.8	-2.0
			3/5	114.1	105.0	4.2	2.7	9.1	1.5
			4/7	110.1	104.8	4.4	1.2	5.3	3.2

FIGURE 1. FLYING TEST BED FOR MODEL PROP-FANS

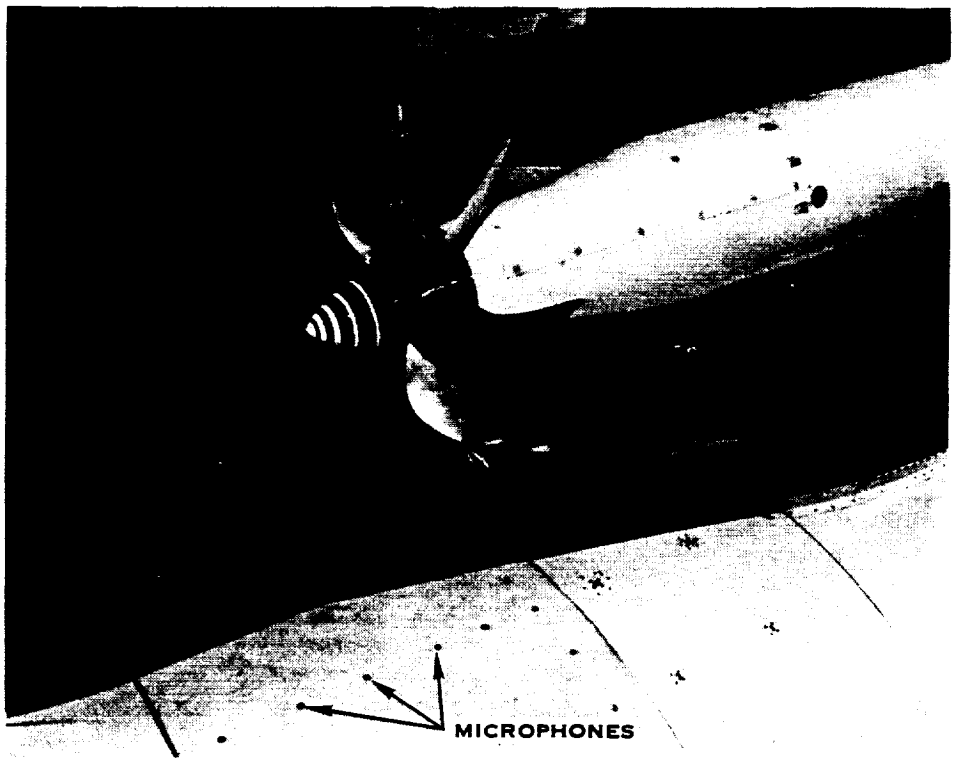

FIGURE 2. PROP-FAN MODEL SR-3 MOUNTED ON JETSTAR BUSINESS AIRCRAFT SHOWING MICROPHONE ARRAY

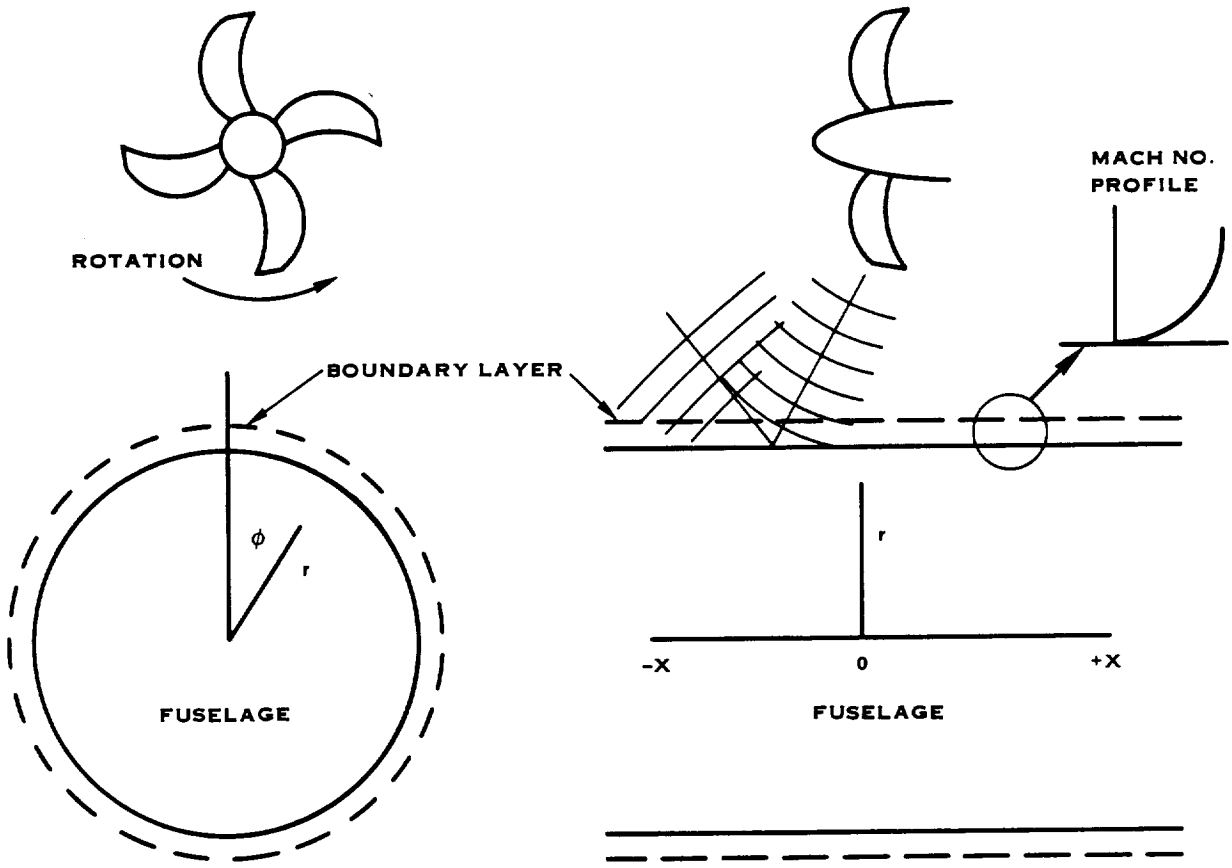

FIGURE 3. GEOMETRY TREATED IN ANALYSIS

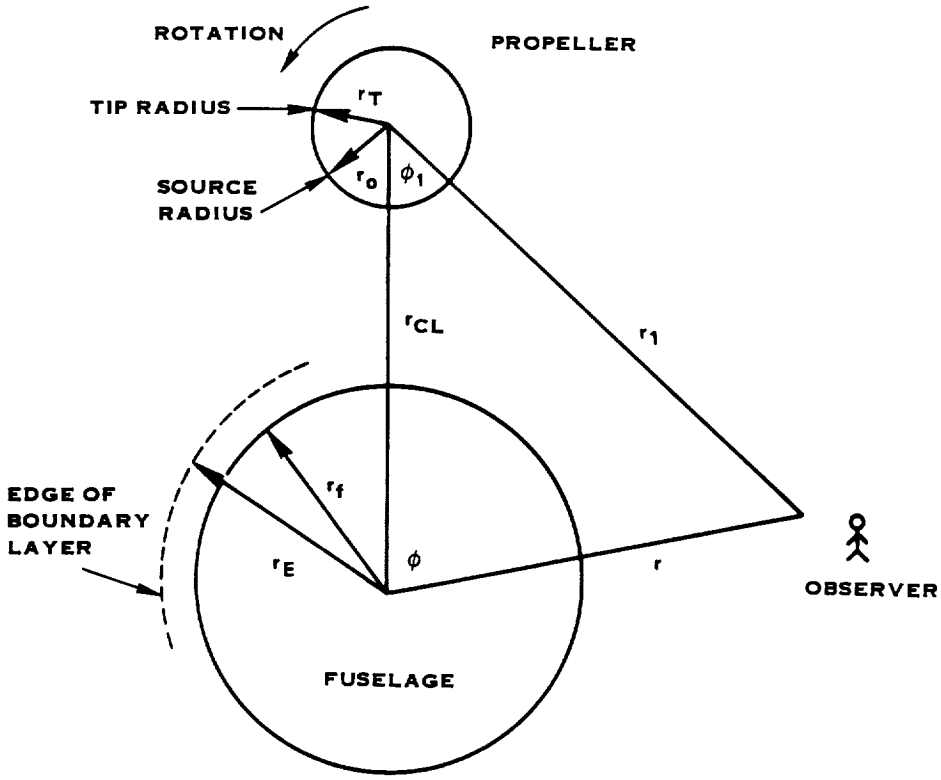

FIGURE 4. SHIFT OF COORDINATE SYSTEM FROM PROPELLER AXIS TO FUSELAGE AXIS

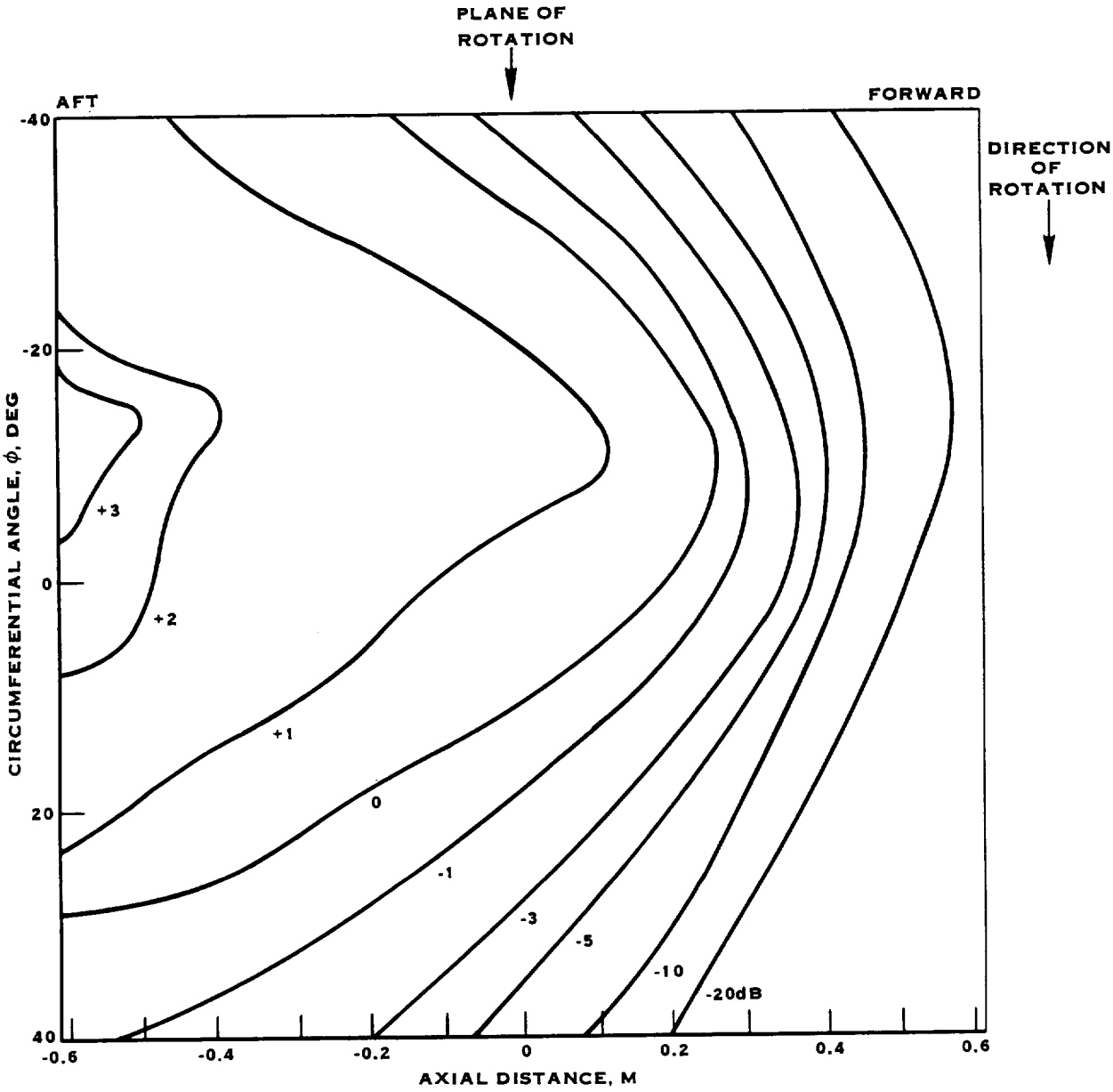

NOTE: CORRECTION FACTORS ARE VALUES TO BE ADDED TO FREE FIELD PREDICTIONS TO OBTAIN LEVELS EXPECTED ON THE FUSELAGE SURFACE.

$M_X = 0.787$
$M_T = 0.816$

FIGURE 5. SAMPLE CALCULATED CORRECTION FACTORS FOR THE JETSTAR FUSELAGE AT BLADE PASSAGE FREQUENCY FOR AN EIGHT BLADE PROP-FAN

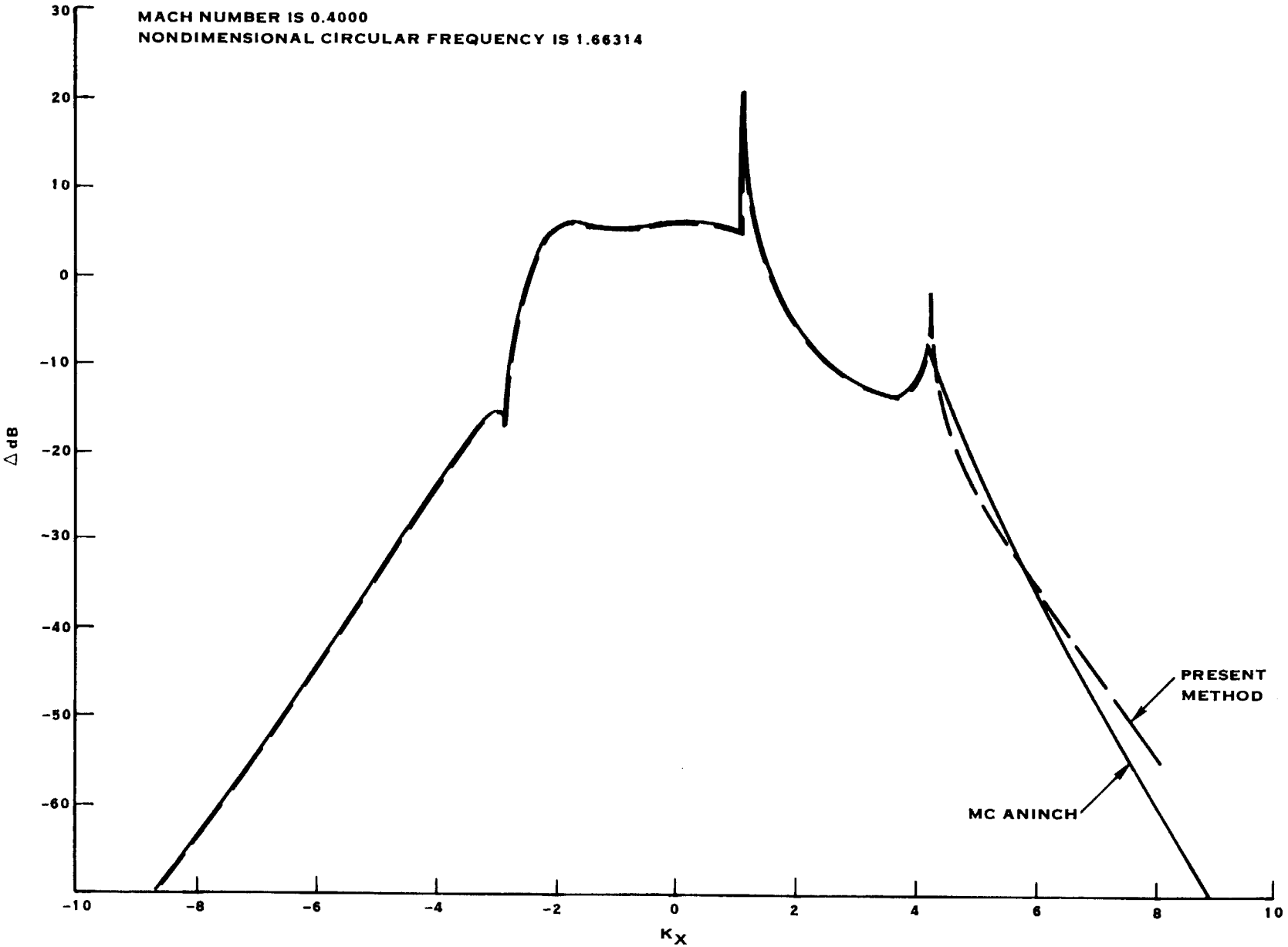

FIGURE 6. COMPARISON OF 2-D AMPLITUDE RESULTS – MC ANINCH VS. PRESENT METHOD

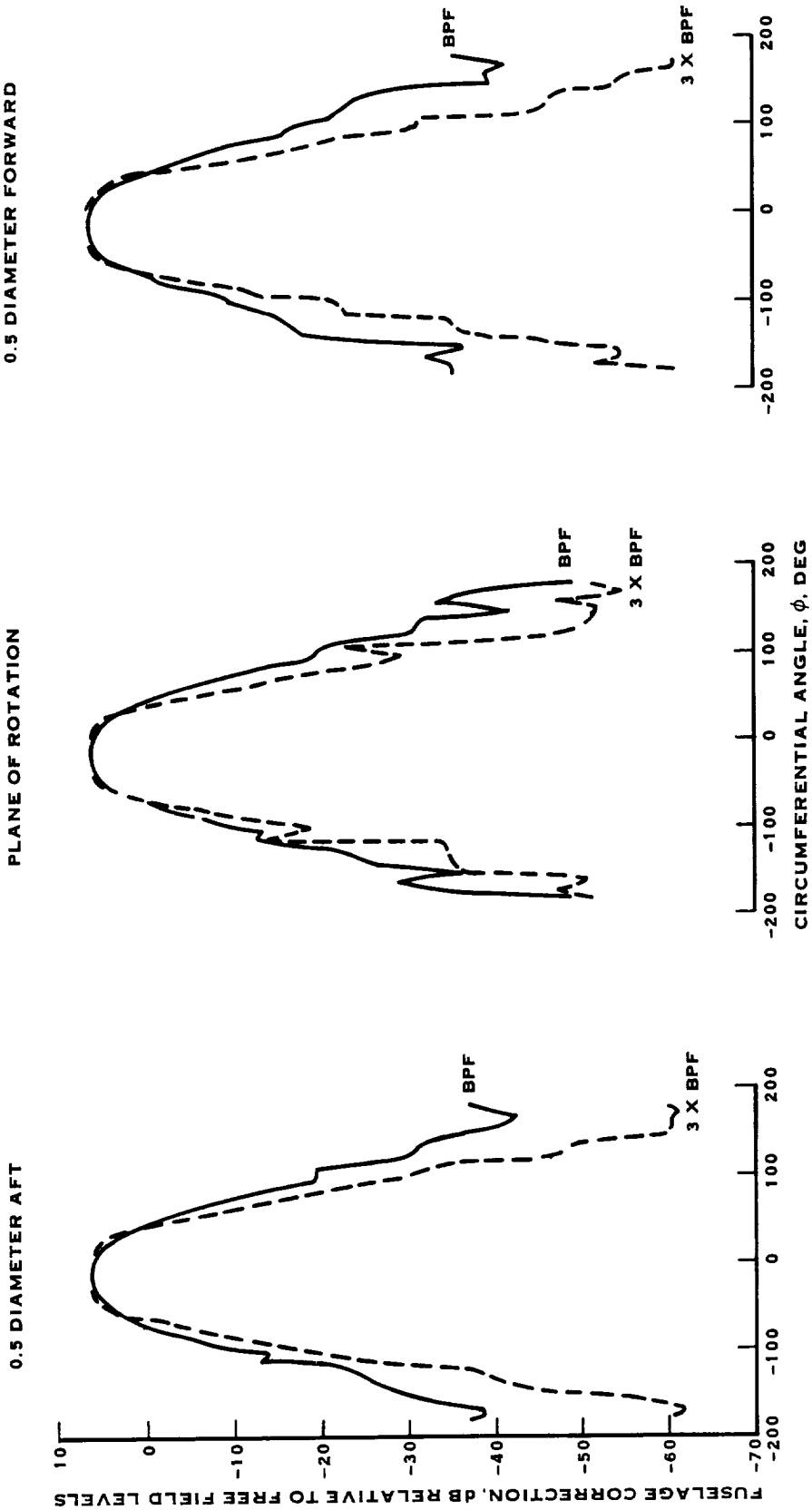

FIGURE 7. CALCULATED FUSELAGE SCATTERING EFFECTS AT $M_X = 0.8$

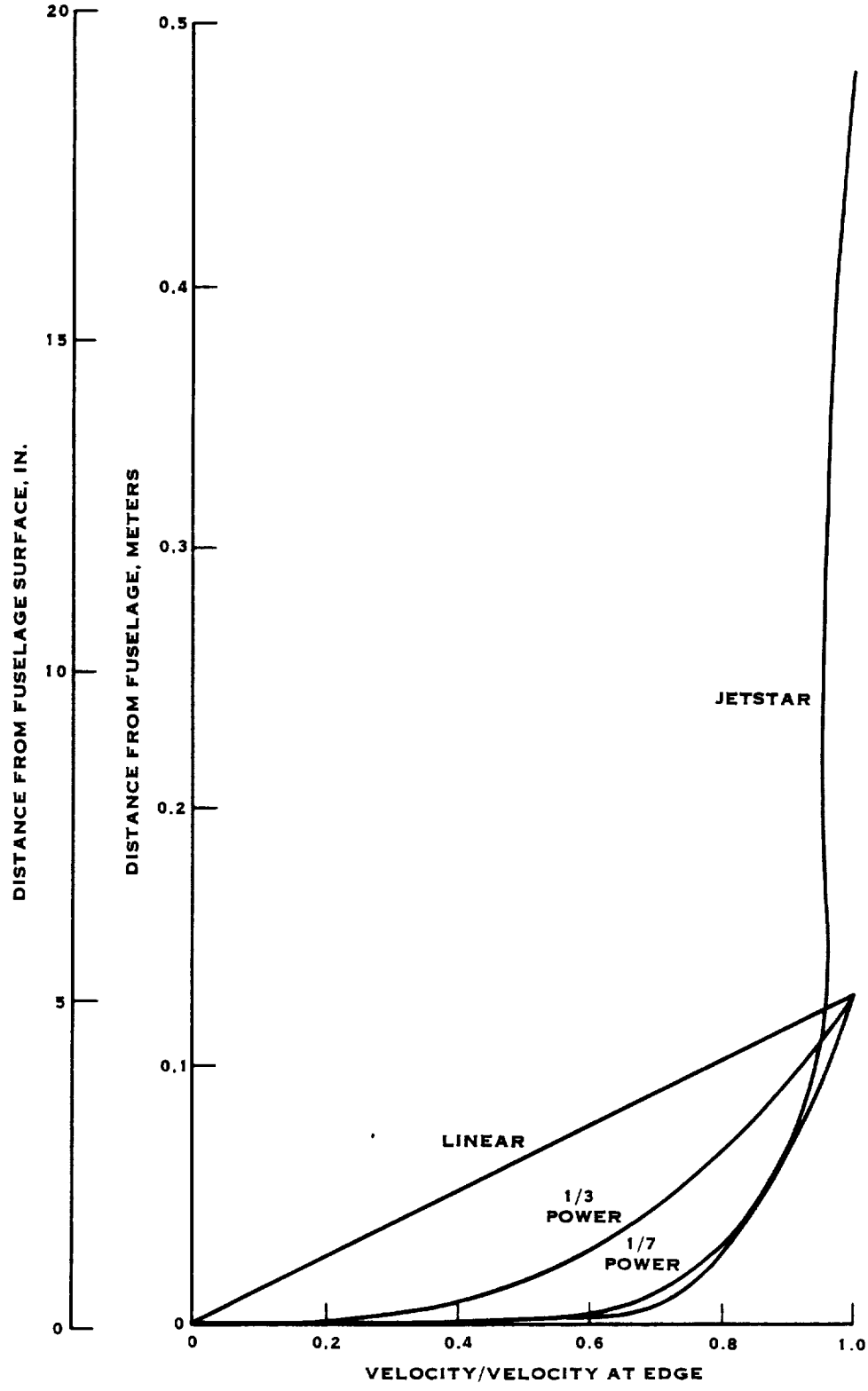

FIGURE 8. SAMPLE BOUNDARY LAYER PROFILES

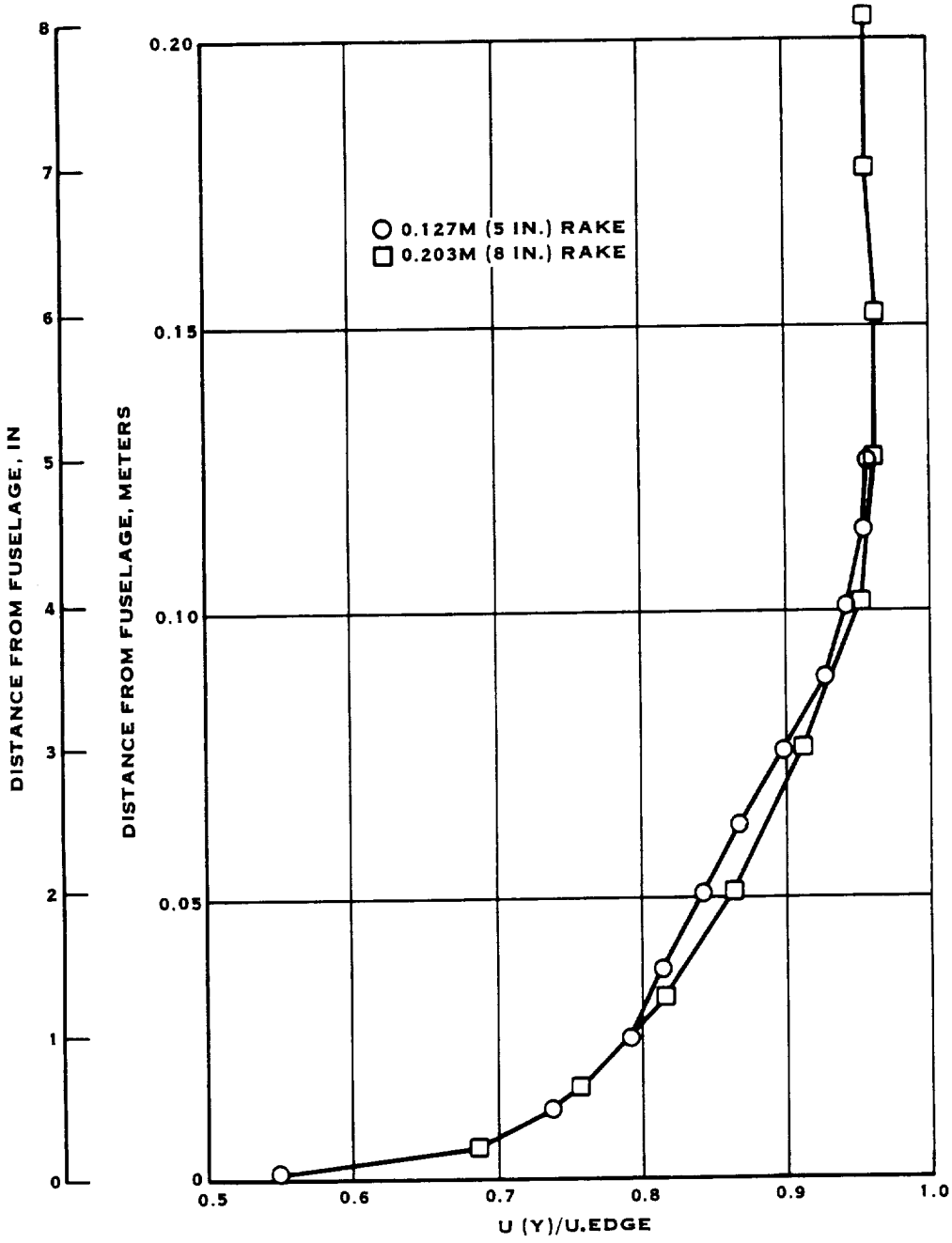

FIGURE 9. MEASURED JETSTAR BOUNDARY LAYER PROFILE AT 0.79 MN

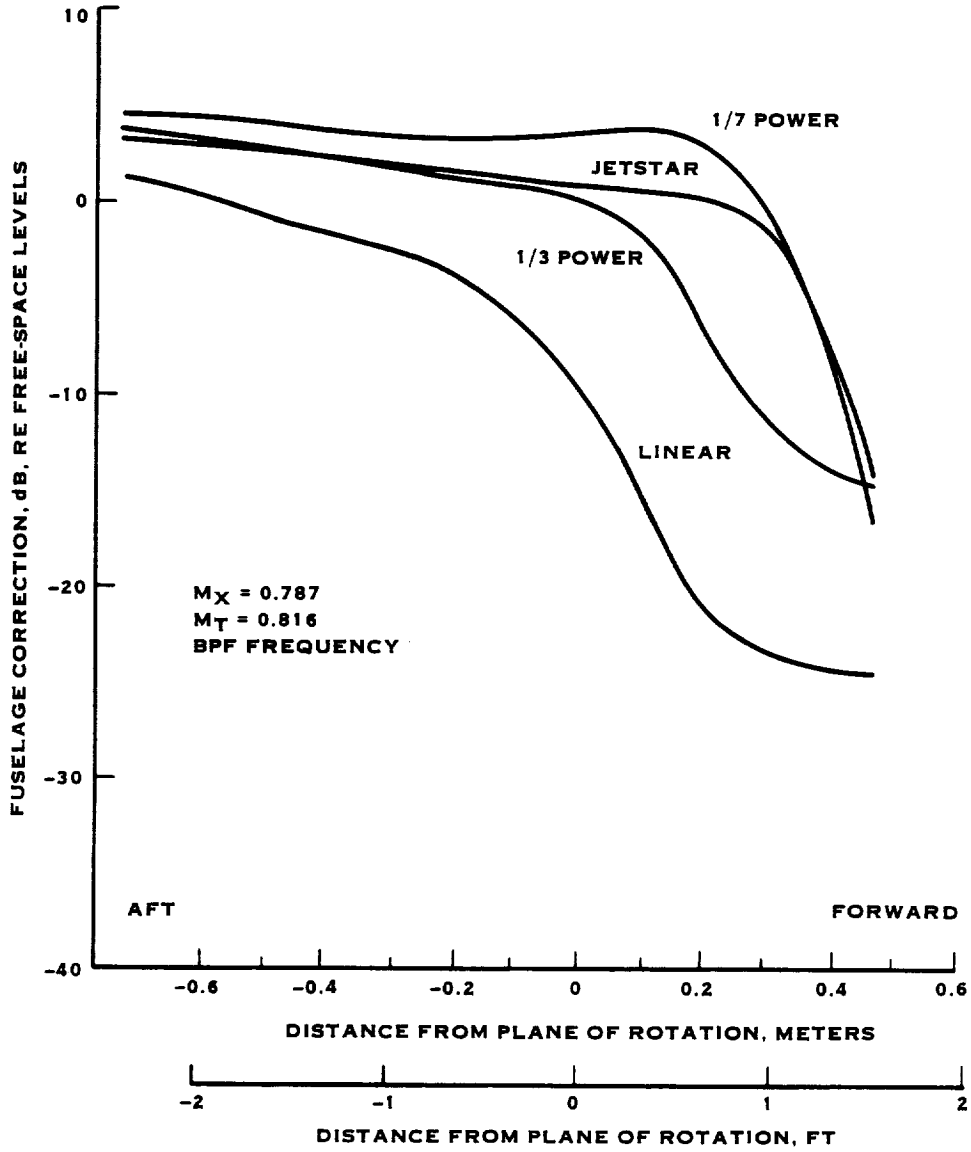

FIGURE 10. EFFECT OF BOUNDARY LAYER PROFILE ON NOISE PROPAGATION TO THE FUSELAGE

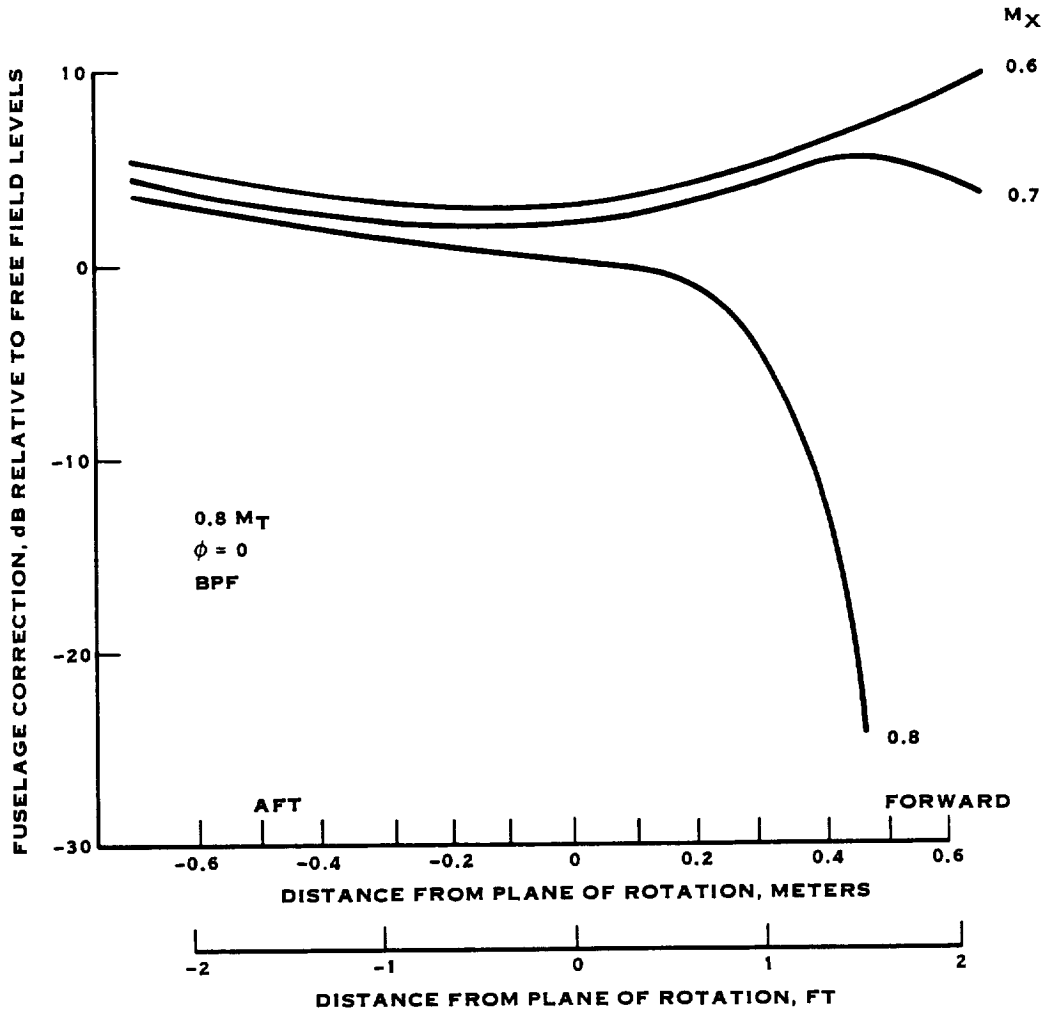

FIGURE 11. BOUNDARY LAYER/FUSELAGE EFFECTS VS. FLIGHT MACH NUMBER AT BLADE PASSING FREQUENCY

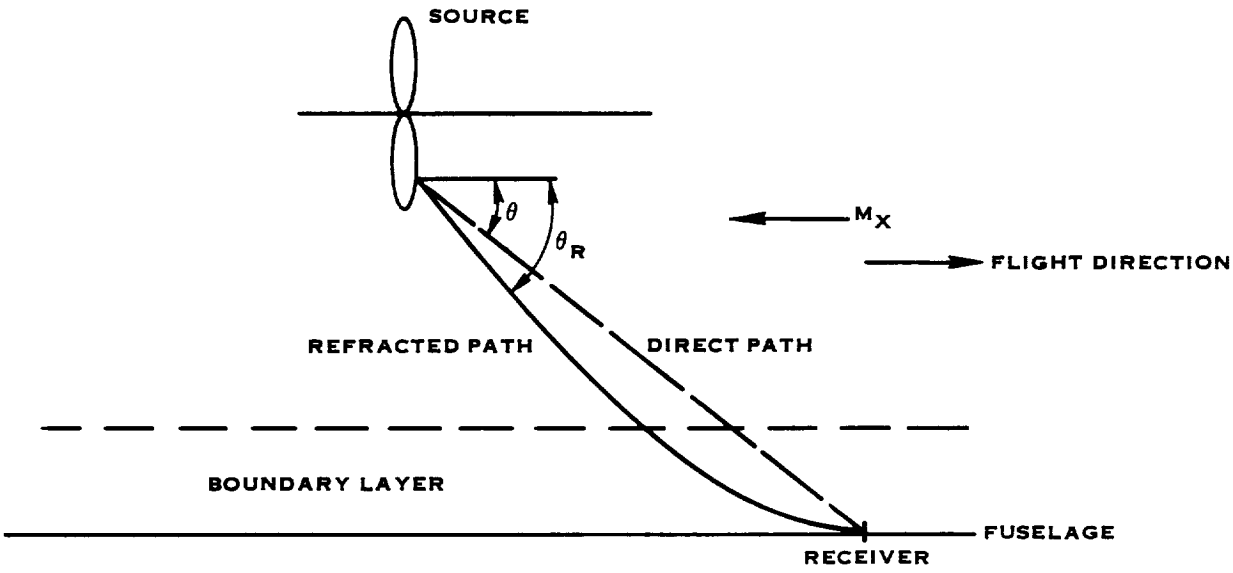

FIGURE 12. ACOUSTIC RAY PROPAGATION THROUGH THE BOUNDARY LAYER

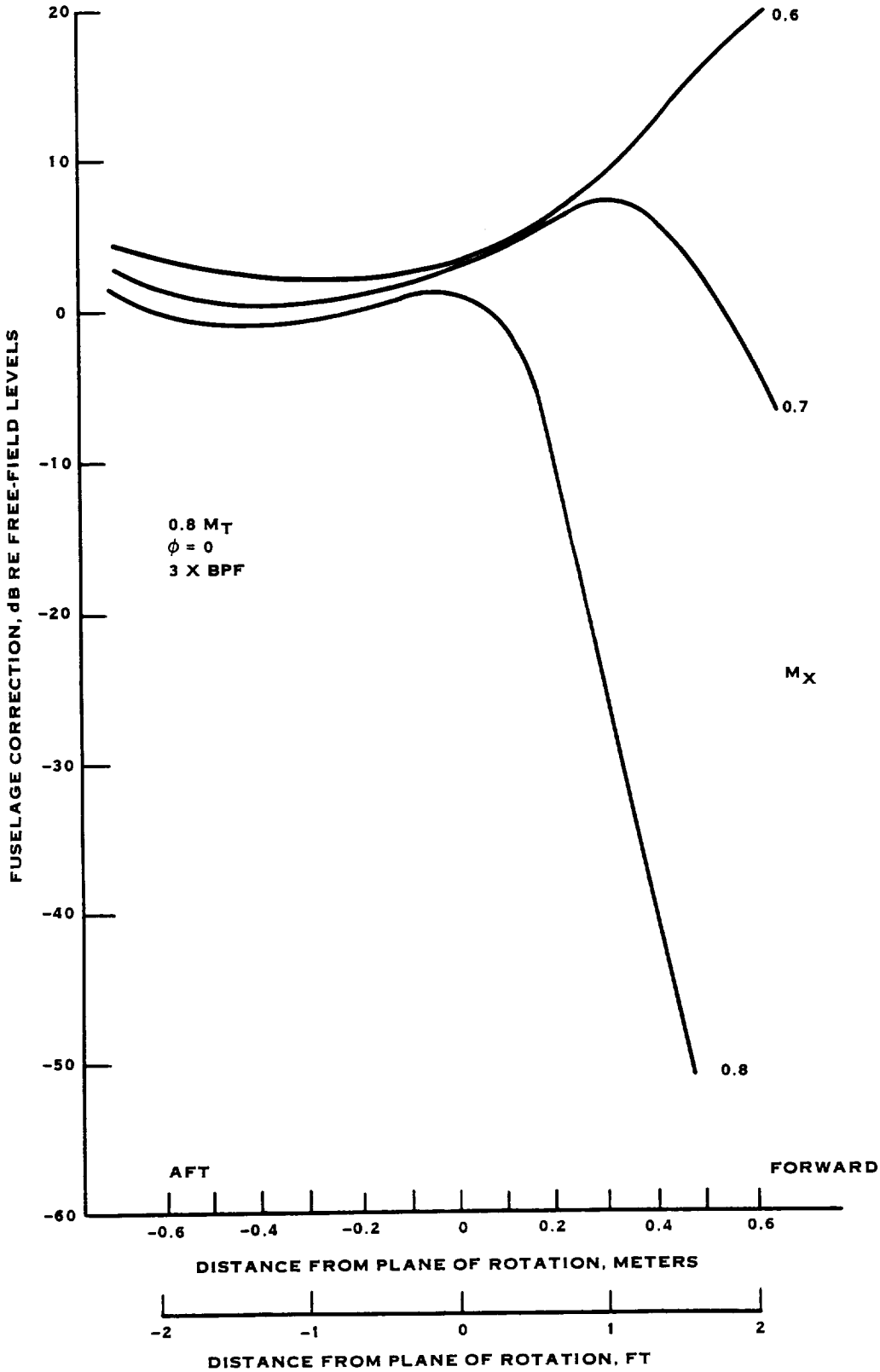

FIGURE 13. BOUNDARY LAYER/FUSELAGE EFFECTS VS. FLIGHT MACH NUMBER AT 3 X BPF

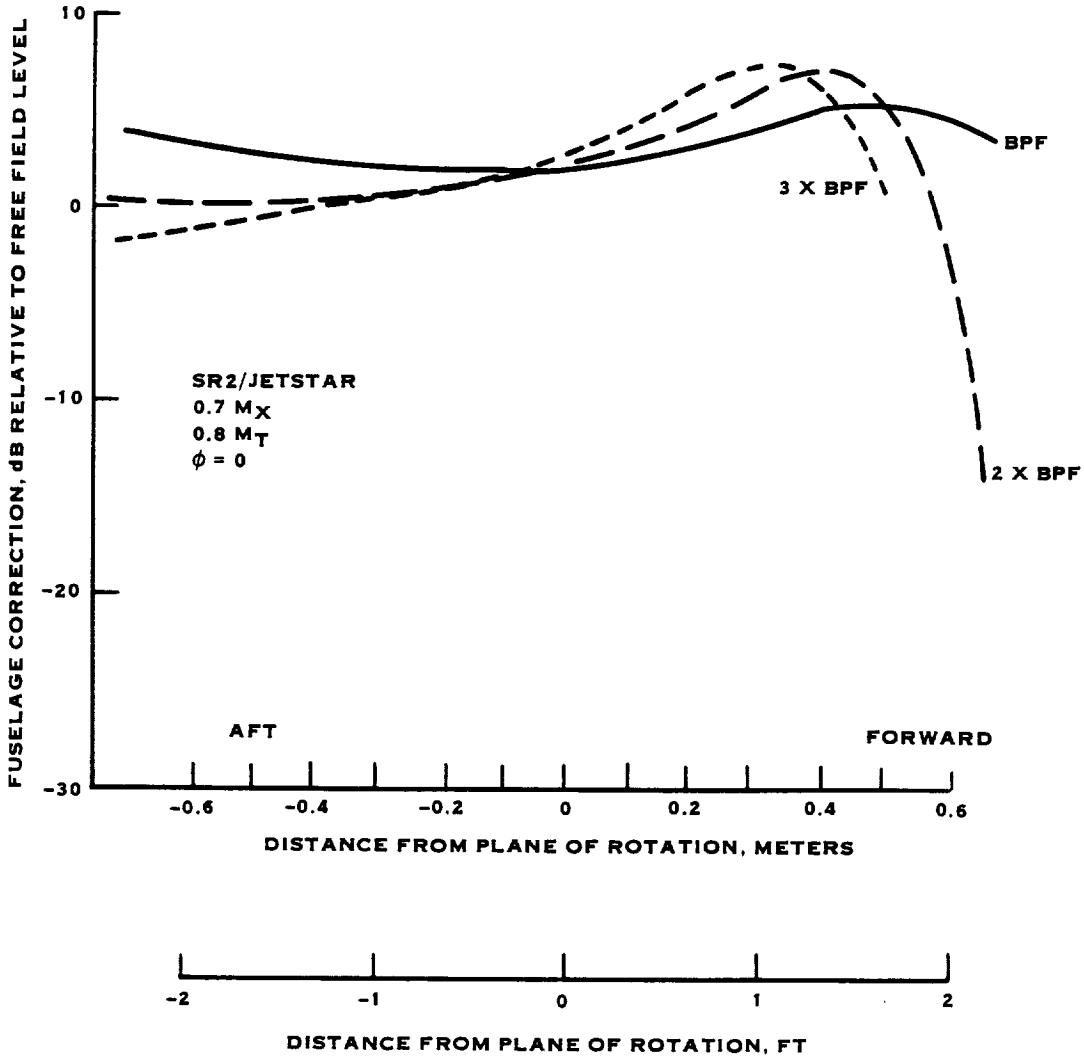

FIGURE 14. BOUNDARY LAYER/FUSELAGE EFFECTS VS. FREQUENCY

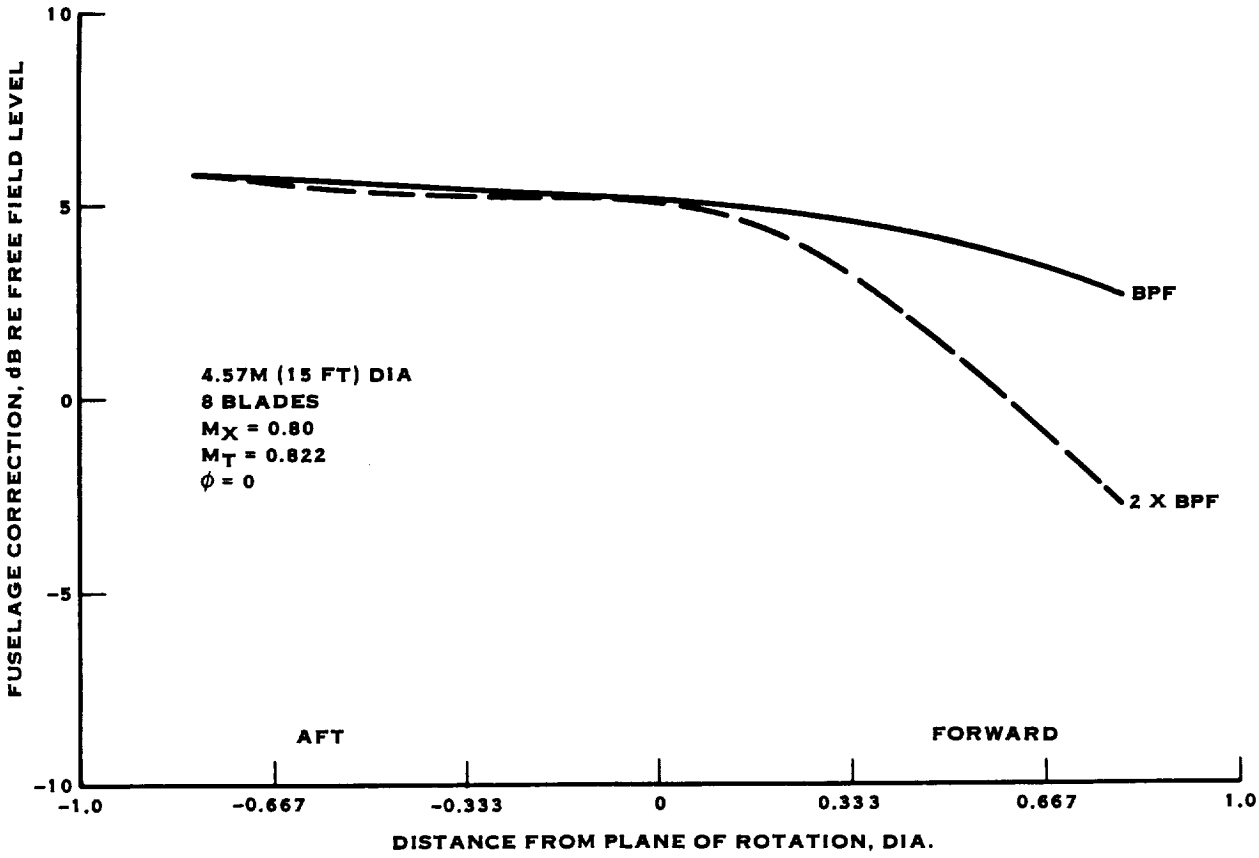

FIGURE 15. FUSELAGE/BOUNDARY LAYER EFFECTS FOR A FULL-SCALE CONFIGURATION

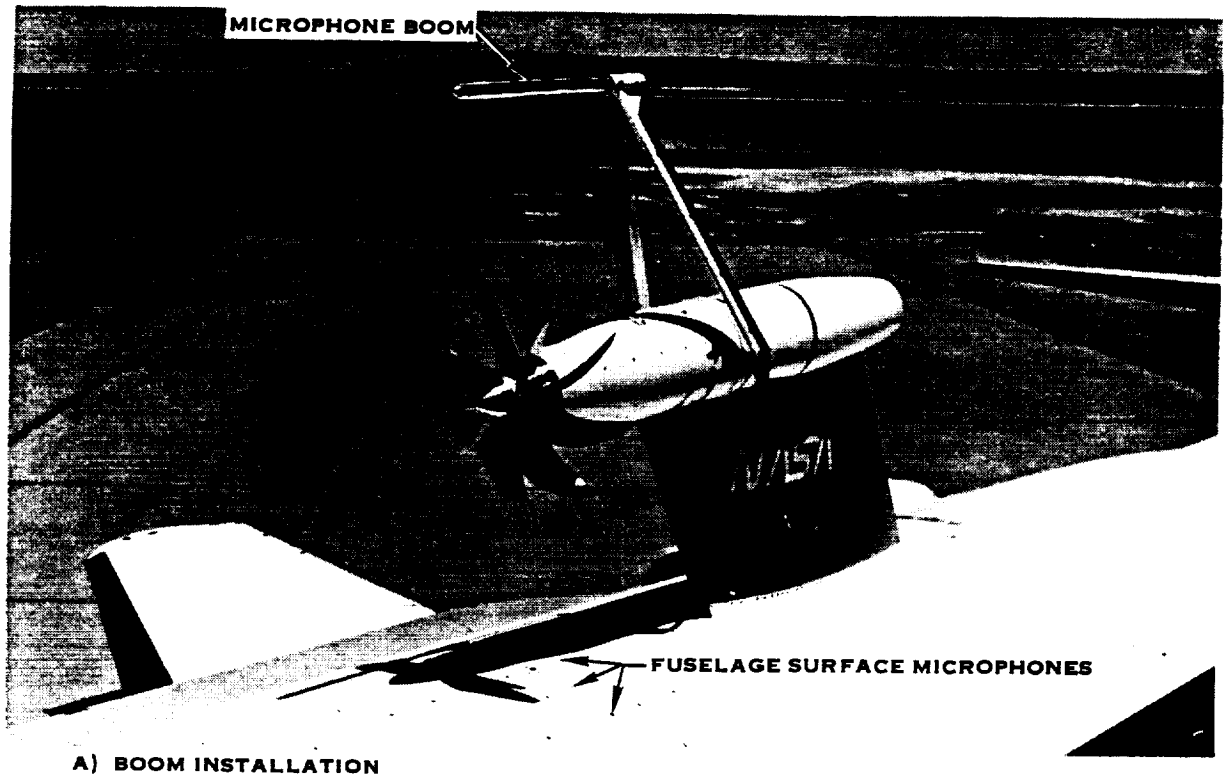

A) BOOM INSTALLATION

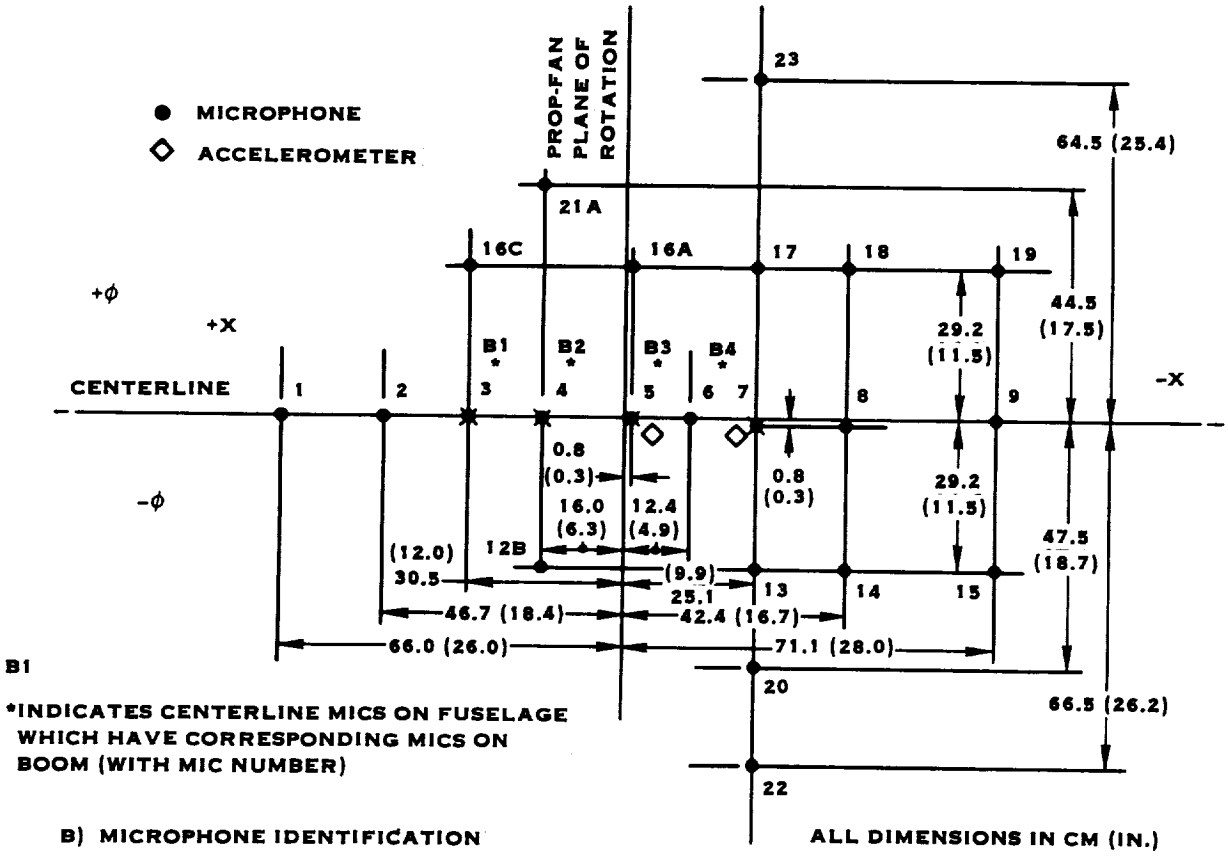

B) MICROPHONE IDENTIFICATION

ALL DIMENSIONS IN CM (IN.)

FIGURE 16. JETSTAR MICROPHONE ARRANGEMENT

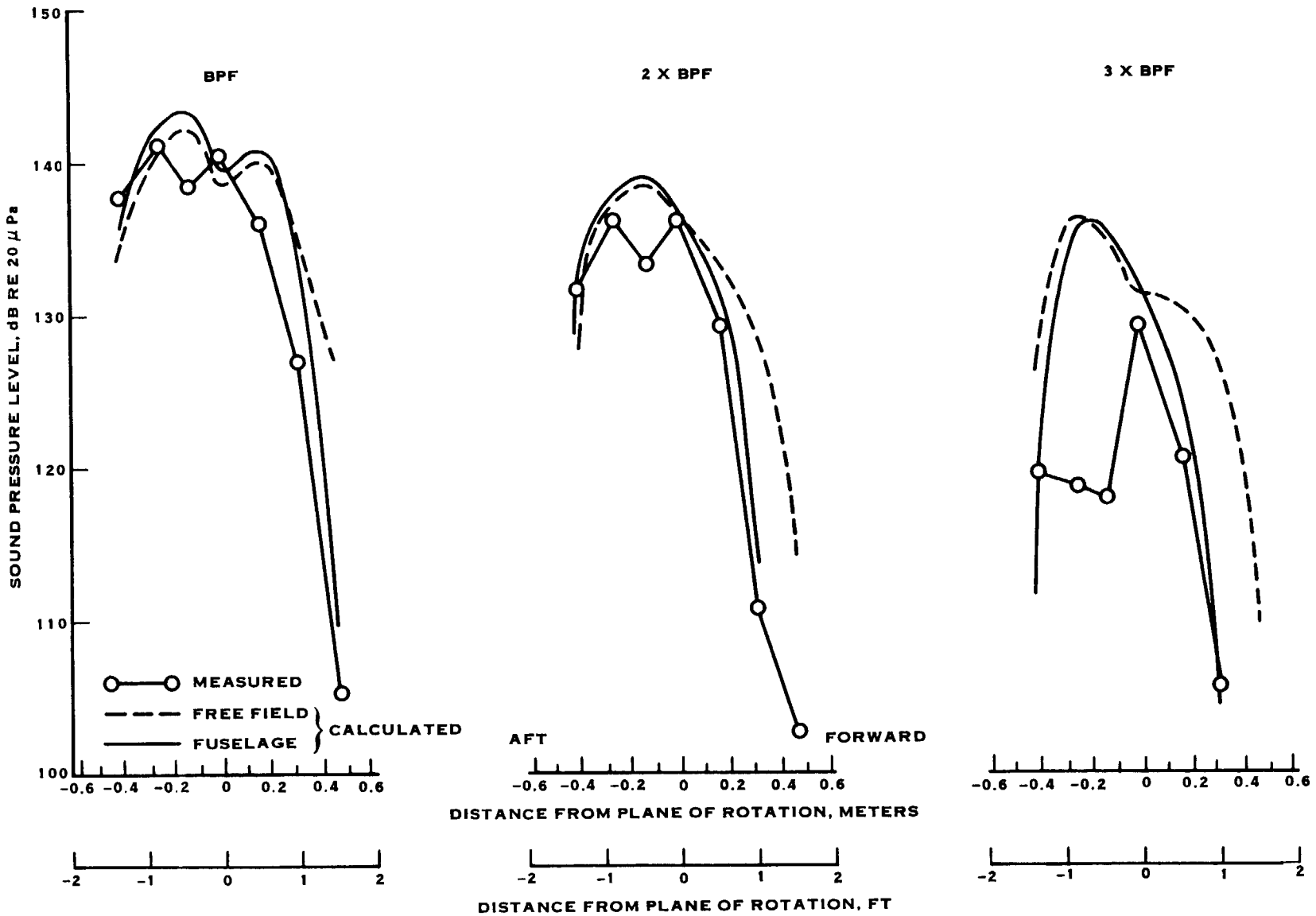

FIGURE 17. COMPARISON OF MEASURED AND CALCULATED SOUND PRESSURE LEVELS AT THE JETSTAR FUSELAGE FOR SR3 AT 0.787 MACH NUMBER

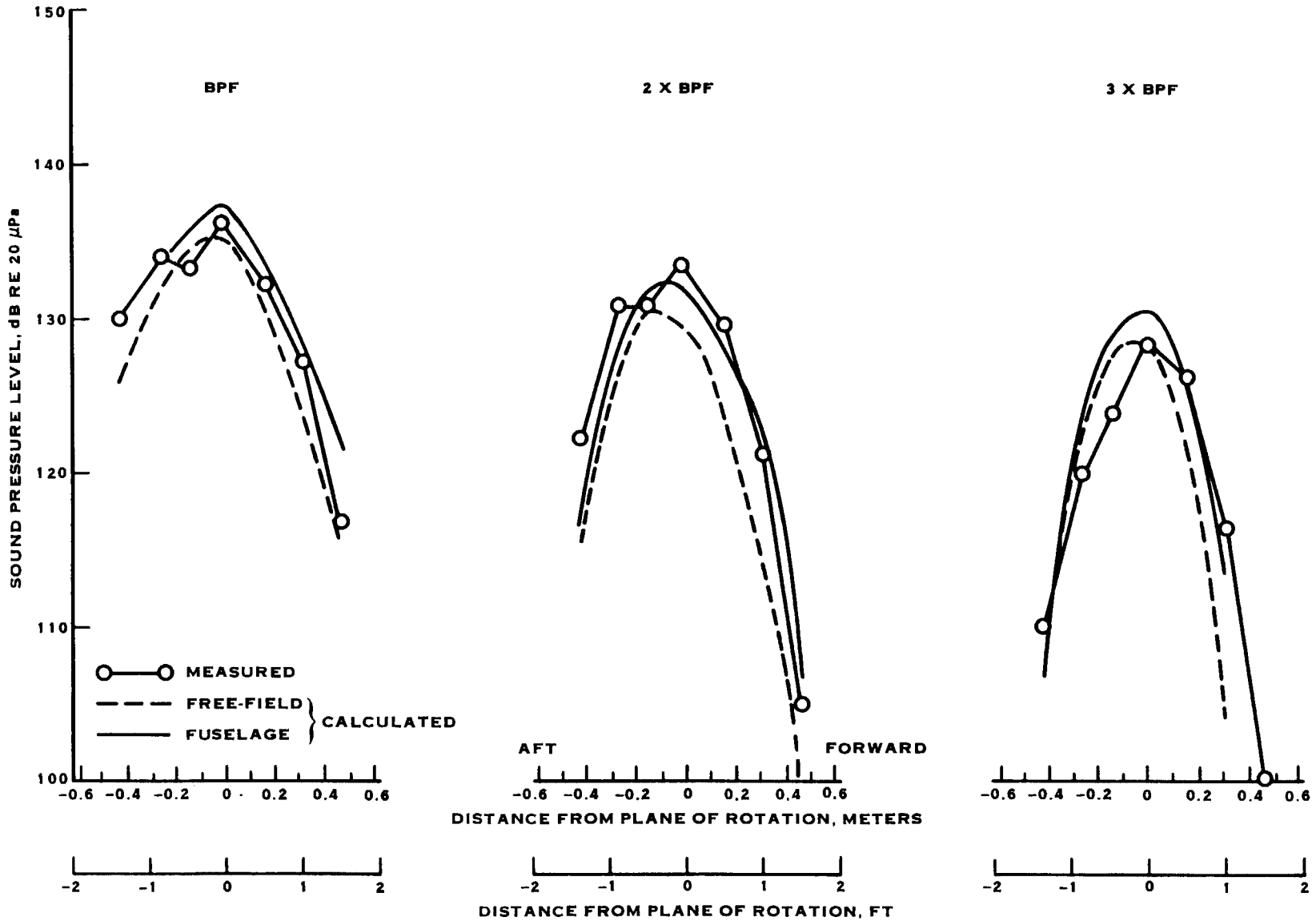

FIGURE 18. COMPARISON OF MEASURED AND CALCULATED SOUND PRESSURE LEVELS AT THE JETSTAR FUSELAGE FOR SR3 AT 0.713 FLIGHT MACH NUMBER

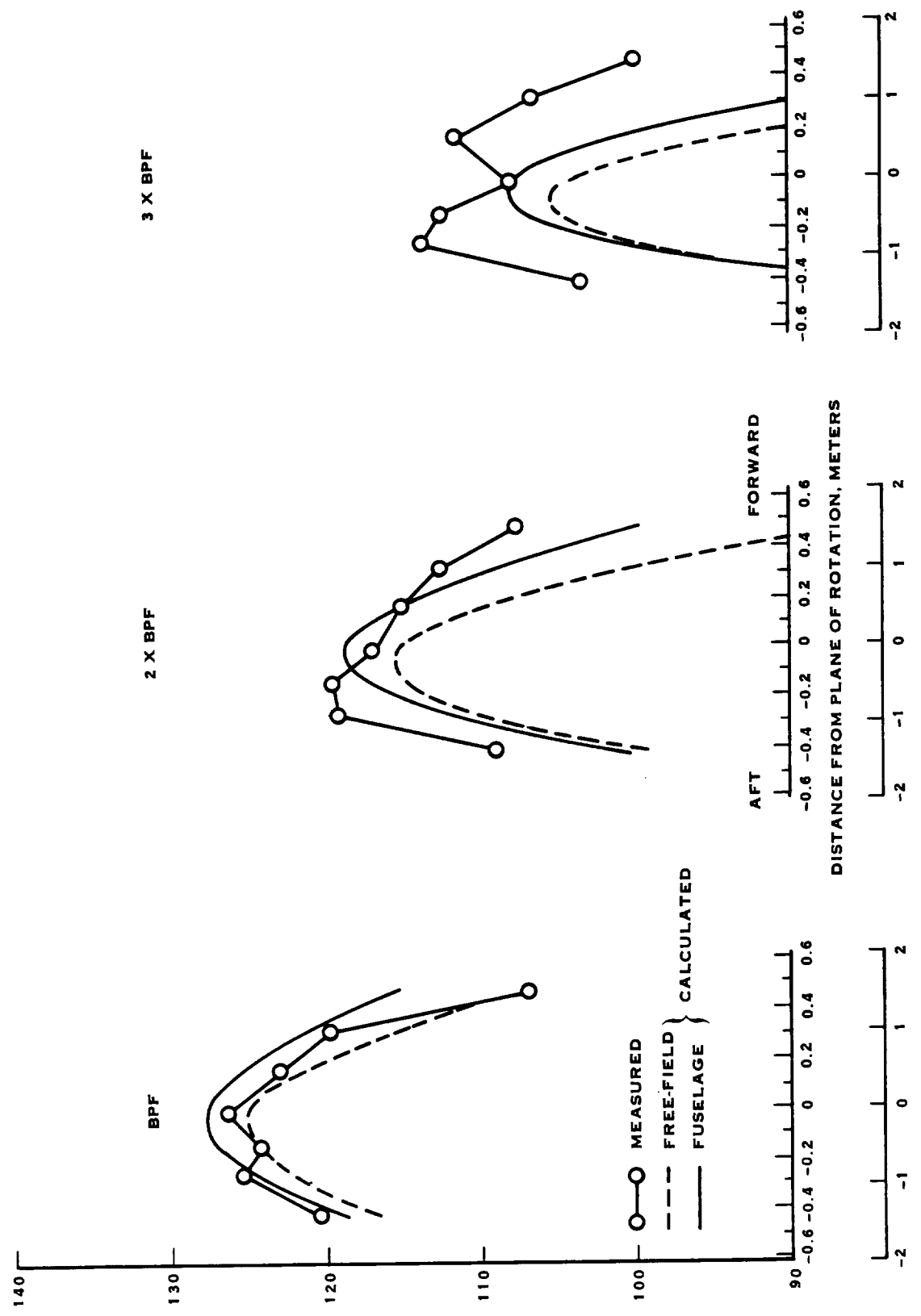

FIGURE 19. COMPARISON OF MEASURED AND CALCULATED SOUND PRESSURE LEVELS AT THE JETSTAR FUSELAGE FOR SR3 AT 0.620 FLIGHT MACH NUMBER

APPENDIX A - JETSTAR FUSELAGE MICROPHONE CORRECTION FACTORS

This appendix contains the fuselage scattering/boundary layer propagation effects corrections for the existing SR2/SR3 eight-bladed models tested on the JetStar airplane. These corrections are based on the present analysis and are presented as dB increments to be added to free-field levels to correct them to fuselage surface noise levels. Alternately, the correction factors can be subtracted from the JetStar fuselage microphone measurements to correct them to free-field conditions.

The correction factors are presented as an array, with columns corresponding to axial positions on the fuselage (positive forward from the plane of rotation) and rows corresponding to circumferential angles on the fuselage. Figure A-1 identifies the microphone positions on the fuselage for which the correction factors were calculated. Note that there are more correction factors given than there are actual microphone positions, since the array of correction factors is complete whereas microphone at corner locations were not used.

The tables of correction factors are presented in the following sequence:

Table No.	Flight Mn.	Rotational Mn
1	0.60	0.60
2	0.60	0.70
3	0.60	0.80
4	0.70	0.60
5	0.70	0.70
6	0.70	0.80
7	0.80	0.60
8	0.80	0.70
9	0.80	0.80

Each table provides corrections for the first three harmonics of blade passing frequency (i.e. 8P, 16P, and 24P harmonics, with P = RPM/60). Although the data may not match the operating conditions of the tables exactly, correction factors using linear interpolation in Mach number should be adequate.

The correction factors given are applicable to both SR2 and SR3 in their 8-bladed configuration and can also be used for the 20,000 ft altitude and 30,000 ft altitude data.

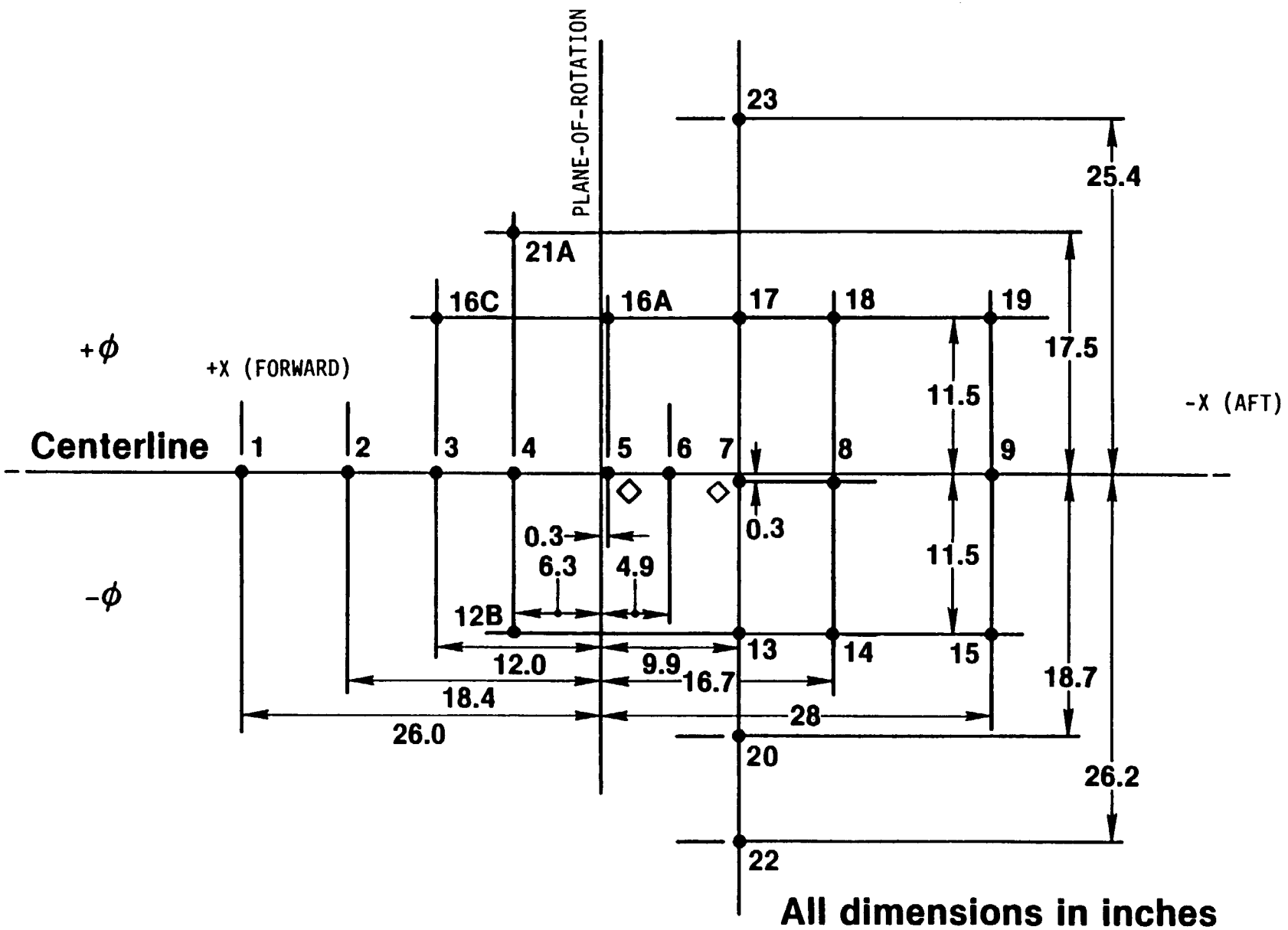

Figure A-1 JetStar Fuselage Microphone Locations

TABLE A-1 JETSTAR FUSELAGE CORRECTIONS FOR M_X=0.6 and M_T=0.6

BOUNDARY LAYER AND FUSELAGE REFLECTION DB CORRECTION FOR HARMONIC NO. 1

VISUAL DISTANCE, FT

PHI, DEG	-2.333	-1.392	-0.825	-0.408	-0.025	0.525	1.000	1.533	2.167
-35.32	6.8	1.4	2.3	2.6	2.8	3.2	3.7	5.0	6.9
-25.21	4.7	2.8	3.0	3.0	3.2	3.7	4.6	6.1	8.2
-15.50	11.3	1.6	2.5	2.8	3.1	3.8	5.0	7.2	9.7
0.0	10.8	3.5	2.0	2.2	2.6	3.6	5.4	8.1	10.1
15.50	10.5	-0.3	2.0	2.1	2.2	2.8	3.8	5.2	8.5
23.59	6.8	-0.1	1.6	1.7	1.7	2.1	2.7	3.2	5.2
34.24	2.0	-0.2	-0.1	0.1	0.2	0.5	0.9	1.4	2.5

BOUNDARY LAYER AND FUSELAGE REFLECTION DB CORRECTION FOR HARMONIC NO. 2

VISUAL DISTANCE, FT

PHI, DEG	-2.333	-1.392	-0.825	-0.408	-0.025	0.525	1.000	1.533	2.167
-35.32	6.7	1.2	2.5	2.7	3.1	4.1	5.4	7.3	10.0
-25.21	13.9	1.2	3.0	2.9	3.3	4.6	6.4	9.1	13.0
-15.50	14.5	2.6	2.5	2.8	3.3	4.9	7.2	11.1	16.4
0.0	27.5	4.8	1.8	2.1	2.8	5.0	8.3	13.3	20.9
15.50	21.5	-0.6	1.3	1.2	1.9	3.9	6.7	10.2	15.0
23.59	12.8	-0.1	0.6	0.8	1.3	2.8	4.6	6.6	6.5
34.24	7.3	0.8	-1.1	-0.5	0.0	0.7	1.2	1.7	0.8

BOUNDARY LAYER AND FUSELAGE REFLECTION DB CORRECTION FOR HARMONIC NO. 3

VISUAL DISTANCE, FT

PHI, DEG	-2.333	-1.392	-0.825	-0.408	-0.025	0.525	1.000	1.533	2.167
-35.32	-5.3	2.1	2.0	2.2	2.9	4.5	6.7	9.3	12.5
-25.21	11.7	2.5	2.1	2.4	3.2	5.1	7.9	11.9	17.2
-15.50	23.7	3.0	2.0	2.5	3.3	5.7	9.1	14.6	22.9
0.0	42.4	4.4	0.8	1.8	2.9	6.1	10.9	18.6	28.8
15.50	35.4	3.6	-0.6	0.8	1.9	4.9	8.7	14.6	21.7
23.59	22.0	-1.1	-0.2	0.4	1.3	3.6	6.2	8.4	5.1
34.24	8.8	-1.1	-1.3	-0.8	-0.2	0.8	1.3	0.9	1.5

TABLE A-2 JETSTAR FUSELAGE CORRECTIONS FOR M_X=0.6 and M_T=0.7

BOUNDARY LAYER AND FUSELAGE REFLECTION DB CORRECTION FOR HARMONIC NO. 1

VISUAL DISTANCE, FT

PHI, DEG	-2.333	-1.392	-0.825	-0.408	-0.025	0.525	1.000	1.533	2.167
-35.32	3.3	2.6	2.9	2.8	2.9	3.3	3.8	4.5	6.0
-25.21	-17.1	4.5	3.2	3.0	3.1	3.8	4.8	5.9	7.0
-15.50	3.3	3.7	3.3	3.2	3.3	4.0	5.1	6.7	9.2
0.0	3.8	4.8	2.8	2.6	2.8	3.8	5.4	7.5	9.7
15.50	5.4	1.6	1.7	1.9	2.1	2.7	3.7	5.5	7.4
23.59	-0.4	2.1	1.8	1.6	1.7	2.2	2.9	3.8	4.4
34.24	2.3	0.3	1.2	1.2	1.2	1.2	1.3	1.0	0.5

BOUNDARY LAYER AND FUSELAGE REFLECTION DB CORRECTION FOR HARMONIC NO. 2

VISUAL DISTANCE, FT

PHI, DEG	-2.333	-1.392	-0.825	-0.408	-0.025	0.525	1.000	1.533	2.167
-35.32	7.0	3.0	2.2	2.4	2.8	3.8	5.1	6.8	8.4
-25.21	7.1	1.5	2.9	2.9	3.2	4.5	6.1	8.7	11.7
-15.50	18.0	1.8	2.9	2.9	3.3	4.7	6.9	10.6	15.2
0.0	22.4	0.4	2.6	2.4	2.9	4.9	7.9	12.2	18.1
15.50	11.5	1.8	1.3	1.6	2.2	3.8	6.2	9.2	11.7
23.59	6.2	-0.0	0.9	1.1	1.6	2.8	4.3	5.4	6.1
34.24	-6.7	-0.3	0.6	0.5	0.7	1.2	1.6	0.8	-3.9

BOUNDARY LAYER AND FUSELAGE REFLECTION DB CORRECTION FOR HARMONIC NO. 3

VISUAL DISTANCE, FT

PHI, DEG	-2.333	-1.392	-0.825	-0.408	-0.025	0.525	1.000	1.533	2.167
-35.32	1.0	2.3	1.9	2.2	2.9	4.3	6.2	8.2	9.4
-25.21	16.5	1.3	2.4	2.5	3.2	5.0	7.5	11.2	15.9
-15.50	14.5	2.9	2.3	2.6	3.3	5.5	8.7	13.9	20.3
0.0	27.9	0.6	1.7	2.1	3.0	5.8	10.3	17.0	26.7
15.50	21.8	0.5	0.7	1.3	2.2	4.8	8.0	12.2	18.4
23.59	15.5	-0.5	0.2	0.6	1.4	3.3	5.4	6.9	3.0
34.24	7.1	-0.1	-0.9	-0.4	0.1	0.7	0.3	-1.8	-4.4

TABLE A-3 JETSTAR FUSELAGE CORRECTIONS FOR M_X=0.6 and M_T=0.8

BOUNDARY LAYER AND FUSELAGE REFLECTION DB CORRECTION FOR HARMONIC NO. 1

VISUAL DISTANCE, FT

PHI, DEG	-2.333	-1.392	-0.825	-0.408	-0.025	0.525	1.000	1.533	2.167
-35.32	2.0	3.2	2.8	2.7	2.8	3.2	3.7	4.4	4.8
-25.21	2.1	3.1	2.7	2.9	3.1	3.5	4.4	5.7	6.8
-15.50	7.4	2.1	3.1	3.3	3.4	3.9	4.7	6.5	8.7
0.0	9.0	3.7	3.2	2.9	3.0	3.8	5.2	6.9	9.9
15.50	5.8	1.9	2.5	2.5	2.5	3.1	3.8	4.8	6.3
23.59	6.3	0.5	1.9	2.0	2.1	2.3	2.6	2.9	4.0
34.24	2.2	1.8	1.6	1.3	1.1	1.3	1.4	1.2	0.4

BOUNDARY LAYER AND FUSELAGE REFLECTION DB CORRECTION FOR HARMONIC NO. 2

VISUAL DISTANCE, FT

PHI, DEG	-2.333	-1.392	-0.825	-0.408	-0.025	0.525	1.000	1.533	2.167
-35.32	-4.4	1.9	2.8	2.6	2.8	3.7	4.8	5.8	6.2
-25.21	9.9	1.9	2.9	2.8	3.2	4.3	5.8	8.0	10.1
-15.50	15.8	1.4	3.1	2.8	3.2	4.5	6.7	9.7	13.4
0.0	18.5	2.7	2.7	2.7	3.0	4.7	7.3	11.5	16.8
15.50	11.5	1.1	1.9	2.1	2.4	3.8	5.7	8.0	9.0
23.59	-1.1	1.0	1.1	1.3	1.8	2.7	3.7	4.5	3.8
34.24	4.7	-0.1	0.7	1.0	1.1	1.3	1.0	-1.5	-9.0

BOUNDARY LAYER AND FUSELAGE REFLECTION DB CORRECTION FOR HARMONIC NO. 3

VISUAL DISTANCE, FT

PHI, DEG	-2.333	-1.392	-0.825	-0.408	-0.025	0.525	1.000	1.533	2.167
-35.32	-19.0	2.3	2.1	2.4	2.9	4.1	5.5	6.9	6.2
-25.21	-2.0	2.6	2.4	2.7	3.3	4.9	7.0	9.9	12.4
-15.50	-13.6	2.4	2.6	2.9	3.5	5.4	8.3	12.8	17.2
0.0	18.9	2.6	2.1	2.5	3.3	5.6	9.5	15.3	20.8
15.50	9.4	1.1	1.2	1.5	2.4	4.5	7.2	9.8	10.8
23.59	12.2	0.6	0.4	1.1	1.8	3.1	4.2	4.7	-2.2
34.24	2.1	-0.2	-0.4	0.1	0.5	0.5	-0.7	-5.0	-9.2

TABLE A-4 JETSTAR FUSELAGE CORRECTIONS FOR M_X=0.7 and M_T=0.6

BOUNDARY LAYER AND FUSELAGE REFLECTION DB CORRECTION FOR HARMONIC NO. 1

PHI, DEG	VISUAL DISTANCE, FT								
	-2.333	-1.392	-0.825	-0.408	-0.025	0.525	1.000	1.533	2.167
-35.32	5.1	1.6	1.6	1.7	1.8	2.4	3.0	3.7	3.3
-25.21	6.3	1.7	1.9	2.0	2.2	3.1	4.2	5.7	6.3
-15.50	5.5	2.3	2.2	2.1	2.4	3.5	5.2	7.3	8.6
0.0	7.9	1.2	1.4	1.6	1.9	3.2	5.2	7.8	9.3
15.50	9.4	0.7	1.1	0.8	0.8	1.7	2.8	3.8	3.4
23.59	4.0	0.3	0.4	0.1	0.1	0.5	0.9	0.8	-1.7
34.24	-7.6	-0.2	-1.3	-1.5	-1.6	-1.7	-2.0	-3.0	-6.3

BOUNDARY LAYER AND FUSELAGE REFLECTION DB CORRECTION FOR HARMONIC NO. 2

PHI, DEG	VISUAL DISTANCE, FT								
	-2.333	-1.392	-0.825	-0.408	-0.025	0.525	1.000	1.533	2.167
-35.32	-0.6	1.1	1.3	1.5	1.9	3.1	4.1	3.8	-3.3
-25.21	-3.5	1.4	1.5	1.6	2.3	4.2	6.5	8.5	5.9
-15.50	16.9	1.1	1.5	1.6	2.3	4.9	8.3	12.0	11.9
0.0	20.9	-0.5	0.8	0.9	1.8	4.8	9.1	13.4	13.6
15.50	5.9	-0.5	-0.5	-0.2	0.5	2.4	4.3	3.8	-1.6
23.59	10.2	-0.1	-1.5	-1.2	-0.7	0.0	-0.1	-4.2	-1.4
34.24	5.7	-2.3	-2.5	-2.3	-2.5	-3.6	-7.3	-26.1	-9.4

BOUNDARY LAYER AND FUSELAGE REFLECTION DB CORRECTION FOR HARMONIC NO. 3

PHI, DEG	VISUAL DISTANCE, FT								
	-2.333	-1.392	-0.825	-0.408	-0.025	0.525	1.000	1.533	2.167
-35.32	10.5	0.9	0.4	0.9	1.7	3.3	4.3	2.4	-9.5
-25.21	14.1	1.5	0.7	1.1	2.2	5.0	8.1	9.8	2.0
-15.50	32.4	2.0	0.7	1.1	2.3	6.1	10.9	15.3	8.1
0.0	29.2	1.1	-0.3	0.2	1.6	6.3	12.3	17.1	14.2
15.50	17.2	-1.4	-1.9	-1.3	-0.1	2.8	4.9	2.7	13.5
23.59	21.7	-4.4	-2.8	-2.1	-1.4	-0.6	-3.0	-17.8	4.1
34.24	2.0	-4.9	-3.5	-3.8	-4.3	-7.0	-16.0	-13.6	-2.3

TABLE A-5 JETSTAR FUSELAGE CORRECTIONS FOR M_X=0.7 and M_T=0.7

BOUNDARY LAYER AND FUSELAGE REFLECTION DB CORRECTION FOR HARMONIC NO. 1

VISUAL DISTANCE, FT

PHI, DEG	-2.333	-1.392	-0.825	-0.408	-0.025	0.525	1.000	1.533	2.167
-35.32	1.1	2.7	1.9	1.7	1.8	2.2	2.5	2.3	0.1
-25.21	2.1	2.7	2.1	2.1	2.2	3.0	3.9	4.6	3.5
-15.50	-6.7	3.1	2.0	2.1	2.3	3.3	4.8	6.4	6.0
0.0	8.6	1.6	2.3	2.0	2.1	3.2	4.9	6.6	6.7
15.50	1.9	1.0	1.1	1.0	1.1	1.6	2.3	2.5	-0.3
23.59	-1.2	-0.0	0.2	0.3	0.3	0.3	0.2	-0.7	-4.4
34.24	2.5	-0.4	-0.1	-0.5	-0.8	-1.4	-2.2	-4.6	-12.6

BOUNDARY LAYER AND FUSELAGE REFLECTION DB CORRECTION FOR HARMONIC NO. 2

VISUAL DISTANCE, FT

PHI, DEG	-2.333	-1.392	-0.825	-0.408	-0.025	0.525	1.000	1.533	2.167
-35.32	1.5	1.3	1.4	1.5	1.8	2.5	2.5	-0.1	-12.8
-25.21	7.9	1.8	1.6	1.7	2.2	3.8	5.3	5.5	-4.0
-15.50	7.3	1.8	1.7	1.7	2.4	4.5	7.1	9.3	3.5
0.0	16.6	2.4	1.1	1.3	2.0	4.5	7.8	10.2	2.9
15.50	9.4	0.7	0.1	0.4	0.9	2.2	2.9	-0.4	-6.1
23.59	9.8	-0.8	-0.4	-0.5	-0.3	-0.2	-1.6	-9.3	-8.4
34.24	3.4	-1.9	-1.7	-1.8	-2.3	-4.4	-10.1	-23.7	-21.6

BOUNDARY LAYER AND FUSELAGE REFLECTION DB CORRECTION FOR HARMONIC NO. 3

VISUAL DISTANCE, FT

PHI, DEG	-2.333	-1.392	-0.825	-0.408	-0.025	0.525	1.000	1.533	2.167
-35.32	3.9	0.6	0.7	1.0	1.6	2.4	1.5	-5.0	-19.7
-25.21	-5.2	0.7	1.0	1.4	2.3	4.4	6.1	4.0	-4.3
-15.50	-1.9	1.1	1.0	1.4	2.5	5.6	9.2	9.7	-6.0
0.0	31.7	-1.0	0.3	0.8	2.0	5.8	10.2	10.5	6.9
15.50	22.3	-2.1	-0.9	-0.4	0.5	2.4	2.1	-7.4	4.2
23.59	15.1	-2.2	-1.4	-1.3	-1.0	-1.3	-5.3	-15.7	-2.0
34.24	2.3	-2.5	-2.6	-3.1	-4.2	-8.4	-19.6	-19.6	-6.9

TABLE A-6 JETSTAR FUSELAGE CORRECTIONS FOR M_X=0.7 and M_T=0.8

BOUNDARY LAYER AND FUSELAGE REFLECTION DB CORRECTION FOR HARMONIC NO. 1

VISUAL DISTANCE, FT

PHI, DEG	-2.333	-1.392	-0.825	-0.408	-0.025	0.525	1.000	1.533	2.167
-35.32	4.1	1.9	2.0	1.9	1.9	1.9	1.8	0.7	-3.2
-25.21	3.7	2.9	2.1	2.0	2.2	2.7	3.3	3.4	0.5
-15.50	-1.1	2.6	2.5	2.4	2.5	3.2	4.2	5.1	3.3
0.0	6.2	2.4	2.2	2.0	2.1	3.0	4.4	5.4	3.7
15.50	-2.4	1.2	1.7	1.4	1.4	1.6	1.9	0.9	-4.6
23.59	1.1	1.0	1.0	0.8	0.6	0.4	-0.3	-2.6	-11.1
34.24	-0.5	-0.0	-0.4	-0.6	-0.8	-1.9	-3.6	-7.3	-14.2

BOUNDARY LAYER AND FUSELAGE REFLECTION DB CORRECTION FOR HARMONIC NO. 2

VISUAL DISTANCE, FT

PHI, DEG	-2.333	-1.392	-0.825	-0.408	-0.025	0.525	1.000	1.533	2.167
-35.32	0.0	1.6	1.3	1.5	1.7	1.7	0.5	-4.3	-23.7
-25.21	2.7	2.1	1.7	1.9	2.3	3.2	3.8	1.9	-13.5
-15.50	1.2	1.9	1.8	1.9	2.4	4.0	5.8	5.9	-10.0
0.0	-3.2	0.8	1.4	1.6	2.1	4.0	6.3	6.5	-13.4
15.50	10.6	1.1	0.7	0.9	1.2	1.8	1.2	-5.1	-12.2
23.59	-0.9	-0.0	0.3	0.1	0.1	-0.6	-3.4	-17.4	-19.1
34.24	-0.4	-0.6	-1.1	-1.4	-2.1	-5.3	-12.8	-26.7	-17.3

BOUNDARY LAYER AND FUSELAGE REFLECTION DB CORRECTION FOR HARMONIC NO. 3

VISUAL DISTANCE, FT

PHI, DEG	-2.333	-1.392	-0.825	-0.408	-0.025	0.525	1.000	1.533	2.167
-35.32	3.6	1.1	1.0	1.2	1.5	1.2	-1.7	-12.3	-21.5
-25.21	4.0	1.3	1.4	1.8	2.5	3.7	3.7	-2.4	-9.7
-15.50	2.8	1.4	1.6	2.0	2.9	5.1	7.0	3.8	-7.7
0.0	12.4	0.9	0.9	1.6	2.6	5.2	7.7	3.1	-2.5
15.50	15.4	-1.2	-0.1	0.3	1.0	1.6	-0.9	-16.8	-1.4
23.59	8.9	-0.8	-0.9	-0.5	-0.5	-2.4	-9.4	-26.8	-7.4
34.24	-0.9	-1.2	-2.0	-2.6	-3.9	-10.4	-24.1	-24.4	-12.8

TABLE A-7 JETSTAR FUSELAGE CORRECTIONS FOR M_X=0.8 and M_T=0.6

BOUNDARY LAYER AND FUSELAGE REFLECTION DB CORRECTION FOR HARMONIC NO. 1

VISUAL DISTANCE, FT

PHI, DEG	-2.333	-1.392	-0.825	-0.408	-0.025	0.525	1.000	1.533	2.167
-35.32	1.6	0.4	-0.0	-0.4	-0.8	-1.9	-4.6	-12.6	-15.2
-25.21	3.6	1.3	0.6	0.2	0.1	0.1	-1.1	-8.1	-11.8
-15.50	4.6	1.3	0.8	0.3	0.3	1.1	1.0	-4.8	-9.7
0.0	8.2	1.8	0.2	-0.2	-0.3	0.7	0.8	-6.0	-6.8
15.50	2.2	-0.6	-1.2	-1.7	-2.1	-2.7	-5.0	-17.1	-11.4
23.59	3.9	-0.9	-2.1	-2.8	-3.5	-5.2	-9.2	-19.9	-13.4
34.24	-5.3	-2.4	-3.4	-4.4	-5.6	-8.9	-15.0	-20.7	-15.4

BOUNDARY LAYER AND FUSELAGE REFLECTION DB CORRECTION FOR HARMONIC NO. 2

VISUAL DISTANCE, FT

PHI, DEG	-2.333	-1.392	-0.825	-0.408	-0.025	0.525	1.000	1.533	2.167
-35.32	-0.3	-0.6	-1.3	-1.6	-2.3	-6.1	-19.1	-29.6	-37.2
-25.21	3.9	-0.1	-0.7	-0.8	-0.6	-1.3	-8.6	-18.3	-29.8
-15.50	0.3	-0.1	-0.7	-0.7	-0.1	1.1	-2.8	-14.6	-32.3
0.0	19.5	-0.1	-1.3	-1.5	-0.9	0.7	-3.5	-12.7	-25.4
15.50	13.7	-2.1	-3.0	-3.4	-3.7	-6.5	-28.3	-23.9	-14.6
23.59	6.0	-3.1	-3.9	-4.9	-6.4	-13.3	-28.9	-25.9	-17.2
34.24	-1.0	-4.6	-6.6	-8.5	-12.2	-28.9	-27.1	-26.1	-30.7

BOUNDARY LAYER AND FUSELAGE REFLECTION DB CORRECTION FOR HARMONIC NO. 3

VISUAL DISTANCE, FT

PHI, DEG	-2.333	-1.392	-0.825	-0.408	-0.025	0.525	1.000	1.533	2.167
-35.32	1.0	-2.3	-2.6	-3.0	-4.2	-12.0	-25.5	-28.4	-23.1
-25.21	11.4	-1.3	-2.0	-1.8	-1.4	-3.7	-16.6	-36.3	-21.1
-15.50	2.6	-1.7	-1.8	-1.6	-0.4	0.5	-9.7	-24.3	-14.3
0.0	0.2	-1.7	-2.9	-2.6	-1.4	0.1	-11.7	-21.0	-1.8
15.50	-4.6	-3.2	-5.1	-5.2	-5.6	-12.2	-28.1	-19.4	-1.3
23.59	14.6	-5.2	-6.4	-7.3	-9.8	-24.8	-29.5	-21.2	-11.0
34.24	3.6	-9.2	-9.1	-12.3	-19.2	-42.3	-31.8	-26.5	-21.2

TABLE A-8 JETSTAR FUSELAGE CORRECTIONS FOR M_X=0.8 and M_T=0.7

BOUNDARY LAYER AND FUSELAGE REFLECTION DB CORRECTION FOR HARMONIC NO. 1

VISUAL DISTANCE, FT

PHI, DEG	-2.333	-1.392	-0.825	-0.408	-0.025	0.525	1.000	1.533	2.167
-35.32	2.4	0.7	0.2	-0.4	-1.0	-3.2	-8.3	-19.6	-19.4
-25.21	4.0	1.3	0.6	0.3	0.1	-0.9	-4.0	-16.1	-15.0
-15.50	3.4	1.3	0.9	0.6	0.5	0.4	-1.5	-12.9	-13.3
0.0	2.8	1.5	0.6	0.2	0.0	0.1	-1.7	-15.7	-11.8
15.50	-4.6	0.4	-0.4	-1.1	-1.6	-3.3	-8.0	-21.9	-18.8
23.59	0.8	-0.8	-1.3	-2.0	-3.0	-6.1	-13.6	-18.9	-22.8
34.24	-1.7	-2.1	-3.0	-4.1	-5.8	-10.9	-19.7	-21.3	-22.8

BOUNDARY LAYER AND FUSELAGE REFLECTION DB CORRECTION FOR HARMONIC NO. 2

VISUAL DISTANCE, FT

PHI, DEG	-2.333	-1.392	-0.825	-0.408	-0.025	0.525	1.000	1.533	2.167
-35.32	0.2	-0.4	-0.9	-1.5	-2.9	-10.1	-25.4	-31.3	-32.6
-25.21	-0.4	0.3	-0.3	-0.4	-0.6	-3.8	-17.1	-28.6	-35.1
-15.50	-11.4	0.4	-0.1	-0.1	0.1	-0.8	-9.7	-23.6	-28.3
0.0	3.9	0.5	-0.6	-0.7	-0.4	-1.0	-10.6	-22.5	-18.4
15.50	8.2	-1.5	-2.0	-2.2	-3.0	-8.6	-30.0	-27.8	-23.9
23.59	5.6	-2.2	-2.8	-3.8	-5.9	-16.5	-31.1	-41.6	-45.4
34.24	-4.7	-3.3	-5.2	-7.6	-12.5	-31.7	-39.6	-31.7	-35.3

BOUNDARY LAYER AND FUSELAGE REFLECTION DB CORRECTION FOR HARMONIC NO. 3

VISUAL DISTANCE, FT

PHI, DEG	-2.333	-1.392	-0.825	-0.408	-0.025	0.525	1.000	1.533	2.167
-35.32	3.1	-1.4	-1.9	-2.7	-5.2	-18.2	-33.6	-36.6	-35.7
-25.21	-5.5	-1.1	-1.0	-0.9	-1.3	-8.0	-22.9	-43.3	-25.8
-15.50	14.4	-0.6	-0.9	-0.4	0.2	-2.6	-17.2	-40.1	-29.8
0.0	-7.8	-1.7	-1.8	-1.2	-0.4	-2.7	-18.0	-31.6	-8.8
15.50	10.7	-4.3	-3.3	-3.5	-4.7	-16.0	-41.3	-27.0	-15.4
23.59	-0.1	-4.4	-4.7	-5.9	-9.5	-28.7	-37.5	-30.0	-27.4
34.24	3.0	-5.4	-7.7	-11.8	-21.3	-35.8	-37.0	-36.3	-31.3

TABLE A-9 JETSTAR FUSELAGE CORRECTIONS FOR M_X=0.8 and M_T=0.8

BOUNDARY LAYER AND FUSELAGE REFLECTION DB CORRECTION FOR HARMONIC NO. 1

VISUAL DISTANCE, FT

PHI, DEG	-2.333	-1.392	-0.825	-0.408	-0.025	0.525	1.000	1.533	2.167
-35.32	1.4	0.8	0.4	-0.3	-1.3	-4.9	-12.9	-21.6	-23.1
-25.21	2.9	1.5	1.1	0.6	0.1	-1.9	-7.4	-21.6	-24.4
-15.50	2.2	1.9	1.1	0.9	0.6	-0.6	-4.5	-20.4	-21.7
0.0	3.8	2.2	1.1	0.6	0.3	-0.7	-4.4	-24.6	-17.9
15.50	2.8	0.5	0.1	-0.4	-1.2	-4.2	-12.0	-20.3	-19.0
23.59	1.6	0.3	-0.9	-1.4	-2.7	-7.3	-18.4	-22.1	-21.8
34.24	-0.5	-1.1	-2.1	-3.2	-5.5	-12.7	-27.3	-23.7	-29.5

BOUNDARY LAYER AND FUSELAGE REFLECTION DB CORRECTION FOR HARMONIC NO. 2

VISUAL DISTANCE, FT

PHI, DEG	-2.333	-1.392	-0.825	-0.408	-0.025	0.525	1.000	1.533	2.167
-35.32	0.3	0.1	-0.3	-1.0	-3.4	-14.7	-31.4	-37.9	-43.6
-25.21	3.1	0.7	0.4	0.3	-0.5	-6.9	-24.1	-37.0	-38.3
-15.50	0.5	0.8	0.6	0.7	0.5	-3.4	-17.1	-35.9	-24.9
0.0	12.1	0.7	0.2	0.4	0.3	-3.4	-18.0	-36.8	-18.9
15.50	7.5	-0.4	-0.8	-0.9	-2.2	-11.4	-31.6	-34.1	-27.1
23.59	-5.9	-1.6	-1.5	-2.4	-5.3	-20.2	-36.5	-40.7	-33.2
34.24	-1.9	-2.2	-3.7	-6.4	-12.9	-32.2	-48.0	-43.5	-34.6

BOUNDARY LAYER AND FUSELAGE REFLECTION DB CORRECTION FOR HARMONIC NO. 3

VISUAL DISTANCE, FT

PHI, DEG	-2.333	-1.392	-0.825	-0.408	-0.025	0.525	1.000	1.533	2.167
-35.32	1.5	-0.4	-0.8	-1.7	-6.0	-24.6	-46.5	-45.0	-59.1
-25.21	1.1	0.0	0.2	0.6	-0.8	-13.2	-32.4	-44.1	-38.7
-15.50	7.9	-0.2	0.5	1.5	1.4	-6.5	-24.9	-52.1	-24.5
0.0	7.4	-0.8	-0.2	1.0	1.3	-6.4	-25.3	-50.8	-18.5
15.50	12.0	-1.5	-1.6	-1.2	-3.2	-21.1	-42.6	-38.9	-22.4
23.59	1.8	-2.4	-2.6	-3.5	-8.5	-32.1	-45.1	-43.4	-40.2
34.24	1.2	-3.6	-5.7	-9.6	-20.7	-44.5	-45.9	-46.7	-45.6

APPENDIX B - COMPUTER PROGRAM USER'S GUIDE

Description of User Inputs

The data required to describe the configuration and operating conditions for each case are read and stored into an array labelled DATA. Prior to the run this array is initiated to zero. It is not re-zeroed between cases.

The data required for each case are:

1. A comment line: the case description, for example. This record must not be blank. It is printed at the top of the first page of output.

2. A set of records containing data which are read and interpreted by LOAD, an input handling subroutine.

3. A record with 0 in column 1 and -1. in columns 3 to 5 follows the last data record for each case.

A blank record (in columns 1 to 72) follows the last case to signal the end of the run.

The data records follow the format shown in Figure A-1. Column 1 should contain a number in the range 1 to 5 which indicates the number of data items on this line. Starting in column 3, the location in array DATA of the first data item on the line is input. Data items are then input in floating point format starting in column 13 for the first data item, column 25 for the second, column 37 for the third, column 49 for the fourth, and column 61 for the fifth item. Each item is limited to 12 characters. The order of the data record for each case is not restricted. However, if two or more records contain data for the same location the one that is read last will be used. The 0 -1. record signals the end of the data for each case.

For some data items, defaults have been established. That is, if a specific number in the data array is zero after all the data for the case are read, the number is replaced by the default value. Examples are the starting harmonic, increment in harmonic, and number of harmonic steps. If not specifically input by the user these are set to 1.

The input list is presented in Figure A-2. As noted, locations 4., 10., 11., 12. and 61. to 80. are dimensions which can be input in any consistent set of units (i.e. feet, inches, meters, furlongs, etc.) as they are normalized by the boundary layer thickness. Locations 21. to 60. are in degrees. All other inputs are dimensionless. Unless the user has reasons for doing otherwise it is recommended that the default values be used for locations 81. to 89. Locations 91. to 93. control plotting options. These plots are printer plots and require an IBM 3800 printer with the POH1 character set.

Sample Cases

Two sample cases are provided for the following:

Case 1:

Flight Mach number	0.3	
Altitude	5,000	ft
Number of blades	8	
Prop-Fan radius	4.5	ft
Blade chord/diameter	0.173	
Thickness/chord	0.023	
C.G. alignment/diameter	0.03	
Effective radius	0.8	
Rotational tip speed	800	ft/sec
Fuselage radius	3.9167	ft
Turbulent boundary layer - 1/7 law		
Boundary layer thickness	4	inches
Distance between center-lines	13.958	ft

Case 2:

Flight Mach number	0.8	
Altitude	35,000	ft
Rest same as for Case 1.		

To define the required inputs, it is assumed that for the low altitude case the density ratio is 0.8617 and the speed of sound is 1097 ft/sec, while for the high altitude case the density ratio is 0.3106 and the speed of sound is 972.3 ft/sec.

The general geometry is shown in Figure A-3. This figure shows the relation between the Prop-Fan and the fuselage as well as the direction of rotation and the conventions used for the locations on the fuselage.

The input data set for these cases is given in Figure A-1. The description of the geometry, operating condition, and fuselage locations is given in the first case. Inputs for the harmonics are not given, so the default values will be used, i.e. only the first harmonic will be calculated. For the second case, only the flight Mach number, density ratio, and rotational Mach number are changed from the first case. These new values are thus input to locations 1., 2., and 9., respectively. Finally, location 18. was input a 3. to indicate that three harmonics are to be calculated.

The output from these cases is given in Figure A-4. As shown, the case description is first summarized. Following that is the array of angles and distances for the free-space sound pressure levels. Next, the array for the sound pressure levels on the fuselage are printed. Finally, the array of boundary layer and fuselage corrections in dB is printed. This array is simply the difference between the two previous arrays. Thus, negative values are levels that are below free-field, due to attenuation by the bound-

ary layer or shielding from the fuselage, and positive values are pressure amplification due to the fuselage.

The sequence is repeated for the second case. Here, three sets of arrays are given, one for each of the three harmonics requested.

It should be noted that the magnitude of the calculated sound pressure levels is usually much greater than would normally be calculated or measured. This is a result of using an effective radius monopole source in these calculations. It is not intended that this method be used for estimating noise levels on a fuselage directly. However, since the same source representation is used for calculating both the free-space levels and those on the fuselage, the boundary layer propagation and fuselage scattering effects are properly calculated. These can be applied to fuselage measurements to correct to free-field or to free-field calculations to estimate levels on a fuselage.

It may also be observed that under certain conditions fuselage reflections greater than 6 dB are calculated. As discussed in the main report, this is a consequence of the source directivity.

```
1 3          13          25          37          49          61
n location   item 1      item 2      item 3      item 4      item 5

PTA  5000 FT ALTITUDE    0.3 MACH NUMBER FLIGHT
5 1.         .3          .8617       8.          4.5         .173
5 6.         .023        .03         .8          .729        3.9167
5 11.        .333333     13.95833    4.1428      15.         10.
5 21.        -120.       -90.        -75.        -60.        -45.
5 26.        -30.        -15.        0.          15.         30.
5 31.        45.         60.         75.         90.         150.
5 61.        20.         15.         10.         7.          4.
5 66.        2.          0.          -2.         -5.         -10.
0 -1.
PTA  35000 FT ALTITUDE   0.8 MACH NUMBER FLIGHT
2 1.         .8          .3106
1 9.         .822
1 18.        3.
0 -1.
```

FIGURE A-1. INPUT DATA FORMAT AND SAMPLE CASES

Input list:

Location	Name	Description
1.	mx	Flight Mach number
2.	pp0	Ambient pressure/sea-level standard
3.	b	Number of blades
4.	rt	Tip radius ***
5.	bd	Blade chord/diameter at effective radius
6.	tb	Max thickness/chord at effective radius
7.	cga	Cg (mid-chord) alignment/diameter along advance helix at effective radius
8.	ze	Effective radius/tip radius
9.	mt	Rotational tip Mach number
10.	rf	Fuselage radius ***
11.	delta	Fuselage boundary layer thickness ***
12.	rcl	Distance between rotor and fuselage centerlines ***
13.	iblt	Boundary layer profile: 1. Linear 2. Pohlhausen 3. JetStar (default) 4.xxxx Power law - power = .xxxx
14.	nphi	Number of angles, 0. to 40. Default = 1.
15.	nx	Number of axial locations, 0. to 20. Default = 1.
16.	ms	Start harmonic of BPF. Default = 1.
17.	mi	Increment in harmonic. Default = 1.
18.	mn	Number of harmonic steps. Default = 1.
19.	icalc	Calculation types: 0. Both free-field and thru boundary layer 1. Free-field only 2. Under boundary layer only
21.-60.	phi	Angle(s) around fuselage, degrees
61.-80.	x	Axial distance from plane of rotation, + forward ***
81.	nkxl	No. steps in kx integration over interval -km/(1-mx), km/(1+mx). Program uses nkxl*mb. Default = 10.
82.	npz	No. steps in integration thru boundary layer. Default = 50.
83.	nms	No. steps to stop before singularity in integration thru boundary layer. Default = 2.

*** These inputs can be in any consistent set of units.

FIGURE A-2. DESCRIPTION OF REQUIRED INPUTS

Input list (continued):

Location	Name	Description
84.	ipmain	Printout options from main program 0. Final answers only. 1. Integration limits used. 2. Table of kx and n ranges. 3. Debug.
85.	ipfres	Printout options for free-space calculations 0. No output. 1. No output. 2. Integration limits. 3. Debug.
86.	ipblpr	Printout options for pressures on fuselage surface. 0. No output. 1. Integration limits and singularities. 2. Same as for 1. 3. Debug.
87.	ipblin	Printout options for boundary layer integration. 0. No output. 1. Id of singularity, mesh size, Frobenius coeff. 2. Table of p, dpdz, m, and dmdz vs. z in b.l. 3. Debug.
88.	nlimit	N summation convergence test. Default = 1.E-4.
89.	kxlim	Kx integration convergence test. Default = 1.E-4.
91.	ikxfsp	Not 0. to get plots of free-field wavenumber integr.
92.	ikxblp	Not 0. to get plots of press under b.l. waveno. int.
93.	ipint	Not 0. to get plots of p and dpdz in boundary layer.

FIGURE A-2. (CONCLUDED)

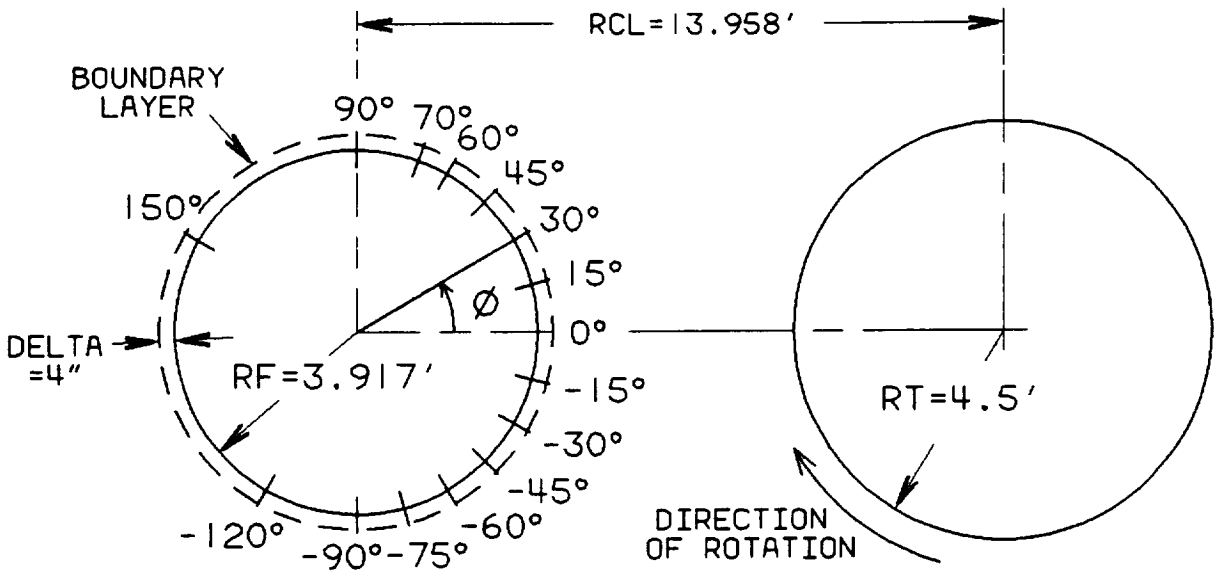

a. CIRCUMFERENTIAL LOCATIONS

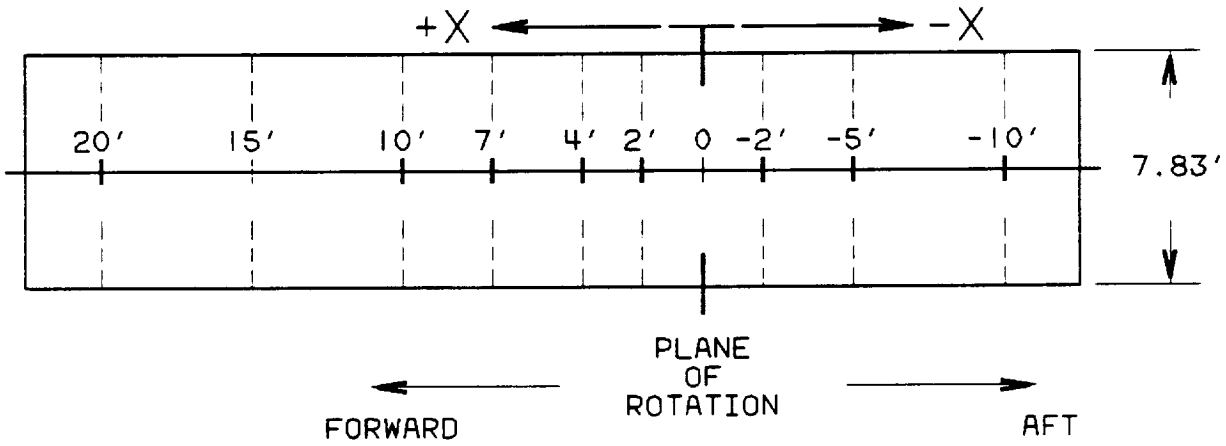

b. AXIAL LOCATIONS

FIGURE A-3. AIRPLANE GEOMETRY AND SIGN CONVENTION.

```
PTA  5000 FT ALTITUDE  0.3 MACH NUMBER FLIGHT

FLIGHT MACH NUMBER =  0.300000        AMBIENT PRESSURE/P0 =  0.861700

BLADE COUNT =    8.                   TIP RADIUS =    4.500          BLADE CHORD/DIA = 0.173000
THICKNESS/CHORD = 0.025000            CG ALIGNMENT = 0.030000        EFFECTIVE RADIUS/TIP RADIUS = 0.800000
ROTATIONAL TIP MACH NO. =  0.729000

FUSELAGE RADIUS =    3.917            BOUNDARY LAYER THICKNESS = 0.333330    CENTERLINE DISTANCE =   13.958
  POWER LAW  BOUNDARY LAYER PROFILE WITH POWER =  0.142800

CIRCUMFERENTIAL ANGLES, DEGREES
 -120.000    -90.000    -75.000    -60.000    -45.000    -30.000    -15.000      0.0       15.000     30.000
   45.000     60.000     75.000     90.000    150.000

AXIAL DISTANCE FROM PLANE OF ROTATION
  20.0000    15.0000    10.0000     7.0000     4.0000     2.0000     0.0       -2.0000    -5.0000   -10.0000


FREE-SPACE SPL FOR HARMONIC NO.     1

                                    VISUAL DISTANCE

PHI, DEG      20.000     15.000     10.000      7.000      4.000      2.000      0.0       -2.000     -5.000    -10.000
 -120.00        94.3      105.5      116.1      121.4      125.0      126.1      126.2      125.0      121.2      111.2
  -90.00        89.7      102.3      114.6      121.8      125.6      127.2      127.3      125.9      121.3      109.3
  -75.00        86.6       99.9      113.4      120.6      125.9      127.8      128.0      126.5      121.3      108.0
  -60.00        83.1       97.2      111.9      119.9      126.2      128.5      128.8      127.1      121.1      106.2
  -45.00        79.3       94.2      110.0      119.1      126.3      129.2      129.7      127.7      120.9      104.3
  -30.00        75.8       91.3      108.2      118.2      126.4      129.8      130.5      128.3      120.5      102.3
  -15.00        73.1       89.1      106.8      117.4      126.4      130.2      131.1      128.7      120.2      100.9
    0.0         72.2       88.3      106.3      117.1      126.4      130.3      131.3      128.8      120.1      100.3
   15.00        73.1       89.1      106.8      117.4      126.4      130.2      131.1      128.7      120.2      100.9
   30.00        75.7       91.3      108.2      118.2      126.4      129.8      130.5      128.3      120.5      102.3
   45.00        79.3       94.2      110.1      119.1      126.3      129.2      129.7      127.7      120.9      104.3
   60.00        83.1       97.2      111.8      119.9      126.2      128.5      128.8      127.1      121.1      106.2
   75.00        86.6       99.9      113.4      120.6      125.9      127.8      128.0      126.5      121.3      108.0
   90.00        89.7      102.3      114.6      121.0      125.6      127.2      127.3      125.9      121.3      109.3
  150.00        96.8      107.2      116.8      121.4      124.5      125.5      125.5      124.4      121.1      112.1

SPL ON THE FUSELAGE FOR HARMONIC NO.     1

                                    VISUAL DISTANCE

PHI, DEG      20.000     15.000     10.000      7.000      4.000      2.000      0.0       -2.000     -5.000    -10.000
 -120.00        96.0      106.6      116.7      121.7      125.0      126.0      126.0      125.0      121.5      112.0
  -90.00        94.7      106.5      118.4      124.6      129.1      130.7      130.8      129.4      124.9      113.1
  -75.00        91.3      104.9      118.3      125.4      130.6      132.4      132.6      131.1      126.0      112.9
  -60.00        88.4      103.1      117.3      125.3      131.4      133.7      134.1      132.4      126.4      111.6
  -45.00        86.0      100.2      115.9      124.8      132.0      134.8      135.3      133.3      126.5      110.0
  -30.00        83.7       97.2      114.4      124.1      132.1      135.4      136.2      134.0      126.3      108.4
  -15.00        80.8       95.5      112.9      123.3      132.1      135.8      136.7      134.3      126.0      106.8
    0.0         75.2       95.2      112.0      122.7      131.8      135.7      136.7      134.3      125.6      105.7
   15.00        79.5       93.8      112.0      122.3      131.3      135.1      136.0      133.6      125.1      105.9
   30.00        82.1       95.2      111.6      121.9      130.4      133.9      134.7      132.4      124.6      105.6
   45.00        71.8       95.9      111.9      121.2      128.9      132.0      132.6      130.6      123.4      106.1
   60.00        84.6       93.9      111.3      120.4      127.2      129.7      130.2      128.4      122.2      106.1
   75.00        84.4       98.0      110.8      118.5      124.6      126.8      127.2      125.6      119.9      105.3
   90.00        78.8       92.3      110.2      117.5      122.5      124.2      124.4      123.1      118.4      105.8
  150.00        92.6       101.4     108.9      112.2      114.3      114.9      114.8      114.0      111.8      105.4

BOUNDARY LAYER AND FUSELAGE REFLECTION DB CORRECTION FOR HARMONIC NO.     1

                                    VISUAL DISTANCE

PHI, DEG      20.000     15.000     10.000      7.000      4.000      2.000      0.0       -2.000     -5.000    -10.000
 -120.00         1.8        1.1        0.6        0.3        0.0       -0.1       -0.1       -0.0        0.3        0.9
  -90.00         5.8        4.2        3.8        3.7        3.6        3.5        3.5        3.5        3.6        3.7
  -75.00         4.7        4.9        5.0        4.8        4.7        4.6        4.6        4.6        4.7        5.0
  -60.00         5.3        6.0        5.5        5.4        5.3        5.2        5.2        5.3        5.3        5.3
  -45.00         6.8        6.1        5.8        5.7        5.6        5.6        5.6        5.6        5.7        5.7
  -30.00         7.9        5.9        6.1        5.9        5.7        5.7        5.7        5.7        5.8        6.1
  -15.00         7.7        6.4        6.1        5.9        5.7        5.6        5.6        5.7        5.8        6.0
    0.0          3.0        6.9        5.8        5.6        5.5        5.4        5.4        5.5        5.5        5.4
   15.00         6.3        4.6        5.1        4.9        4.9        4.9        4.9        5.0        4.9        5.0
   30.00         6.3        3.9        3.3        3.8        4.0        4.1        4.2        4.2        4.0        3.2
   45.00        -7.5        1.7        1.9        2.1        2.6        2.8        2.9        2.8        2.5        1.8
   60.00         1.5       -3.3       -0.6        0.5        1.0        1.2        1.3        1.3        1.0       -0.2
   75.00        -2.2       -1.9       -2.6       -2.0       -1.3       -1.0       -0.9       -0.9       -1.4       -2.7
   90.00       -11.0      -10.0       -4.4       -3.5       -3.1       -2.9       -2.9       -2.8       -2.9       -3.5
  150.00        -4.1       -5.9       -7.9       -9.2      -10.2      -10.6      -10.7      -10.4       -9.3       -6.6
```

FIGURE A-4. SAMPLE CASE OUTPUT.

PTA 35000 FT ALTITUDE 0.8 MACH NUMBER FLIGHT

FLIGHT MACH NUMBER = 0.800000 AMBIENT PRESSURE/P0 = 0.310600

BLADE COUNT = 8. TIP RADIUS = 4.500 BLADE CHORD/DIA = 0.173000
THICKNESS/CHORD = 0.023000 CG ALIGNMENT = 0.030000 EFFECTIVE RADIUS/TIP RADIUS = 0.800000
ROTATIONAL TIP MACH NO. = 0.822000

FUSELAGE RADIUS = 3.917 BOUNDARY LAYER THICKNESS = 0.333330 CENTERLINE DISTANCE = 13.958
POWER LAW BOUNDARY LAYER PROFILE WITH POWER = 0.142800

CIRCUMFERENTIAL ANGLES, DEGREES
-120.000 -90.000 -75.000 -60.000 -45.000 -30.000 -15.000 0.0 15.000 30.000
45.000 60.000 75.000 90.000 150.000

AXIAL DISTANCE FROM PLANE OF ROTATION
20.0000 15.0000 10.0000 7.0000 4.0000 2.0000 0.0 -2.0000 -5.0000 -10.0000

FREE-SPACE SPL FOR HARMONIC NO. 1

VISUAL DISTANCE

PHI, DEG	20.000	15.000	10.000	7.000	4.000	2.000	0.0	-2.000	-5.000	-10.000
-120.00	126.1	140.4	154.9	162.1	166.3	166.6	164.7	161.2	152.9	134.1
-90.00	120.3	135.9	152.4	161.2	166.9	167.7	165.8	161.7	152.0	130.3
-75.00	116.5	132.8	150.4	160.3	167.2	168.4	166.5	162.0	151.2	127.7
-60.00	112.3	129.2	148.1	159.2	167.3	169.2	167.3	162.3	150.2	124.7
-45.00	107.8	125.4	145.4	157.7	167.3	169.9	168.1	162.5	149.0	121.4
-30.00	103.9	121.8	142.9	156.2	167.2	170.5	168.8	162.6	147.7	118.3
-15.00	100.7	119.2	140.9	154.9	167.0	170.9	169.3	162.7	146.8	116.0
0.0	99.9	118.2	140.2	154.4	166.9	171.1	169.5	162.7	146.4	115.1
15.00	100.8	119.2	140.9	154.9	167.0	170.9	169.3	162.7	146.8	116.0
30.00	103.8	121.8	142.9	156.2	167.2	170.5	168.8	162.6	147.7	118.3
45.00	107.8	125.3	145.4	157.7	167.3	169.9	168.1	162.5	149.0	121.4
60.00	112.3	129.2	148.1	159.2	167.3	169.2	167.3	162.3	150.2	124.7
75.00	116.6	132.8	150.4	160.3	167.2	168.4	166.5	162.0	151.2	127.7
90.00	120.3	135.9	152.4	161.2	166.9	167.7	165.8	161.7	152.0	130.3
150.00	129.3	142.9	156.2	162.5	165.8	165.8	164.1	160.8	153.4	136.2

SPL ON THE FUSELAGE FOR HARMONIC NO. 1

VISUAL DISTANCE

PHI, DEG	20.000	15.000	10.000	7.000	4.000	2.000	0.0	-2.000	-5.000	-10.000
-120.00	104.1	117.6	131.7	139.3	146.0	150.3	153.1	153.1	148.3	132.5
-90.00	105.6	121.5	139.1	149.4	158.5	162.5	163.5	161.3	153.2	133.2
-75.00	104.5	121.7	141.0	152.8	163.1	167.1	167.3	164.1	154.3	131.8
-60.00	102.7	120.6	141.6	154.9	166.6	170.6	170.2	166.0	154.5	129.8
-45.00	99.7	118.5	141.1	155.8	168.8	173.0	172.2	167.0	154.0	126.9
-30.00	96.2	115.8	139.6	155.6	169.8	174.5	173.4	167.5	153.1	124.3
-15.00	92.7	112.8	137.6	154.6	169.9	175.1	174.0	167.7	152.2	121.9
0.0	90.0	110.2	135.5	153.0	169.2	175.0	174.1	167.6	151.7	121.1
15.00	87.8	108.3	133.5	151.1	167.7	173.8	173.4	167.3	151.8	121.3
30.00	85.7	106.8	131.8	148.8	165.2	171.6	171.8	166.4	152.0	122.8
45.00	85.4	105.9	130.0	146.1	161.6	168.2	169.1	164.7	151.8	124.3
60.00	84.0	104.6	127.9	142.9	157.0	163.6	165.3	162.1	151.0	125.2
75.00	83.5	103.3	125.3	138.9	151.3	157.9	160.5	158.6	149.4	126.7
90.00	81.7	101.0	121.9	134.1	144.8	151.4	155.0	154.3	147.0	126.4
150.00	82.3	87.8	98.8	109.1	114.3	120.6	130.2	134.6	133.5	112.5

BOUNDARY LAYER AND FUSELAGE REFLECTION DB CORRECTION FOR HARMONIC NO. 1

VISUAL DISTANCE

PHI, DEG	20.000	15.000	10.000	7.000	4.000	2.000	0.0	-2.000	-5.000	-10.000
-120.00	-22.0	-22.8	-23.2	-22.8	-20.3	-16.2	-11.6	-8.1	-4.6	-1.7
-90.00	-14.7	-14.3	-13.3	-11.8	-8.4	-5.2	-2.4	-0.4	1.2	2.9
-75.00	-12.0	-11.1	-9.5	-7.5	-4.0	-1.3	0.8	2.1	3.2	4.1
-60.00	-9.6	-8.6	-6.5	-4.2	-0.8	1.4	2.9	3.7	4.4	5.1
-45.00	-8.2	-6.8	-4.4	-1.9	1.4	3.1	4.1	4.6	5.0	5.6
-30.00	-7.6	-6.0	-3.3	-0.5	2.7	4.0	4.6	4.9	5.3	6.0
-15.00	-8.0	-6.4	-3.3	-0.3	3.0	4.2	4.7	5.0	5.4	6.0
0.0	-9.9	-8.1	-4.7	-1.4	2.4	3.9	4.5	4.9	5.4	6.0
15.00	-13.0	-10.9	-7.4	-3.9	0.7	2.9	4.0	4.6	5.0	5.3
30.00	-18.2	-14.9	-11.1	-7.3	-2.0	1.1	2.9	3.8	4.2	4.5
45.00	-22.4	-19.4	-15.4	-11.5	-5.7	-1.7	1.0	2.2	2.9	2.9
60.00	-28.3	-24.6	-20.1	-16.3	-10.3	-5.6	-2.0	-0.1	0.8	0.5
75.00	-33.0	-29.5	-25.2	-21.4	-15.8	-10.5	-6.0	-3.4	-1.8	-1.0
90.00	-38.6	-34.8	-30.5	-27.1	-22.1	-16.3	-10.9	-7.4	-4.9	-3.9
150.00	-47.0	-55.1	-57.4	-53.3	-51.5	-45.2	-33.8	-26.2	-19.9	-23.7

FIGURE A-4. (CONTINUED).

FREE-SPACE SPL FOR HARMONIC NO. 2

VISUAL DISTANCE

PHI, DEG	20.000	15.000	10.000	7.000	4.000	2.000	0.0	-2.000	-5.000	-10.000
-120.00	100.6	127.8	155.0	168.5	176.4	177.4	175.6	172.0	162.5	135.1
-90.00	90.9	118.4	149.3	165.9	176.5	178.5	176.7	172.5	160.9	128.3
-75.00	75.8	111.9	145.2	163.7	176.4	179.2	177.4	172.8	159.6	123.6
-60.00	81.8	105.4	140.1	160.9	176.1	179.9	178.2	173.0	157.8	118.0
-45.00	80.0	99.1	134.6	157.6	175.5	180.5	179.0	173.2	155.7	111.8
-30.00	79.1	94.1	129.2	154.1	174.6	181.0	179.7	173.3	153.6	106.1
-15.00	78.3	91.0	125.0	151.5	173.9	181.3	180.2	173.3	151.8	102.5
0.0	82.7	82.8	123.6	150.4	173.5	181.4	180.4	173.3	151.2	100.3
15.00	83.8	83.9	125.2	151.5	173.9	181.3	180.2	173.3	151.8	102.1
30.00	79.1	89.2	129.2	154.1	174.6	181.0	179.7	173.3	153.6	105.4
45.00	81.8	98.8	134.6	157.6	175.5	180.5	179.0	173.2	155.7	112.1
60.00	76.8	103.7	140.2	160.9	176.1	179.9	178.2	173.0	157.8	117.9
75.00	82.6	111.9	145.2	163.7	176.4	179.2	177.4	172.8	159.6	123.6
90.00	87.7	118.4	149.3	165.9	176.5	178.5	176.7	172.5	160.9	128.3
150.00	107.1	133.0	157.9	169.7	176.1	176.7	174.9	171.7	163.2	138.7

SPL ON THE FUSELAGE FOR HARMONIC NO. 2

VISUAL DISTANCE

PHI, DEG	20.000	15.000	10.000	7.000	4.000	2.000	0.0	-2.000	-5.000	-10.000
-120.00	80.6	93.0	110.7	131.7	140.4	143.3	143.5	151.7	152.6	132.0
-90.00	79.2	93.6	125.5	143.3	156.5	161.5	166.5	168.6	160.9	130.9
-75.00	72.8	88.9	126.0	146.5	162.6	169.6	174.4	173.6	162.3	127.7
-60.00	79.4	88.1	124.7	147.8	167.4	176.3	179.6	176.5	162.1	123.0
-45.00	80.5	86.8	121.4	147.4	170.6	180.8	182.7	177.8	160.6	117.7
-30.00	75.8	87.5	117.1	145.6	172.1	183.4	184.2	178.1	158.6	112.0
-15.00	75.1	83.4	112.7	142.8	171.8	184.3	184.9	178.2	156.9	107.4
0.0	78.8	81.2	109.5	140.0	170.0	183.6	184.9	178.1	156.2	104.8
15.00	75.7	85.4	106.7	137.9	167.0	181.2	183.9	177.9	156.7	107.2
30.00	66.3	78.8	108.1	136.4	163.4	176.7	181.3	176.9	157.7	110.4
45.00	72.7	80.1	107.3	134.9	159.0	169.9	176.5	174.4	158.1	114.6
60.00	55.9	84.4	106.3	132.5	153.5	162.1	168.9	169.9	157.3	117.7
75.00	76.9	71.6	106.7	128.8	146.7	153.7	158.4	163.2	154.8	120.1
90.00	80.5	77.2	103.5	123.7	138.9	144.5	145.8	154.3	150.9	121.6
150.00	82.2	78.2	77.4	91.7	105.9	108.3	108.2	110.8	125.5	121.3

BOUNDARY LAYER AND FUSELAGE REFLECTION DB CORRECTION FOR HARMONIC NO. 2

VISUAL DISTANCE

PHI, DEG	20.000	15.000	10.000	7.000	4.000	2.000	0.0	-2.000	-5.000	-10.000
-120.00	-19.9	-34.8	-36.3	-36.8	-35.9	-34.0	-32.1	-20.5	-9.9	-3.2
-90.00	-11.7	-24.8	-23.8	-22.6	-20.0	-17.0	-10.2	-3.9	0.0	2.6
-75.00	-3.0	-23.1	-19.1	-17.2	-13.8	-9.6	-3.0	0.8	2.8	4.0
-60.00	-2.4	-17.3	-15.5	-13.1	-8.7	-3.6	1.4	3.5	4.3	5.0
-45.00	0.5	-12.3	-13.2	-10.1	-4.9	0.3	3.7	4.6	4.8	5.9
-30.00	-3.3	-6.6	-12.1	-8.6	-2.6	2.4	4.6	4.8	5.0	5.9
-15.00	-3.2	-7.6	-12.3	-8.7	-2.0	2.9	4.7	4.9	5.1	5.0
0.0	-3.9	-1.5	-14.1	-10.5	-3.5	2.2	4.5	4.8	5.1	4.5
15.00	-8.1	1.5	-18.5	-13.6	-6.8	-0.1	3.7	4.5	4.8	5.2
30.00	-12.8	-10.4	-21.2	-17.8	-11.3	-4.4	1.7	3.6	4.1	5.0
45.00	-9.1	-18.7	-27.3	-22.7	-16.5	-10.6	-2.5	1.2	2.4	2.5
60.00	-20.9	-19.3	-33.9	-28.4	-22.6	-17.8	-9.3	-3.1	-0.5	-0.3
75.00	-5.6	-40.3	-38.5	-34.9	-29.7	-25.4	-19.8	-9.6	-4.7	-3.5
90.00	-7.2	-41.1	-45.8	-42.1	-37.7	-34.0	-30.9	-18.2	-10.0	-6.8
150.00	-24.8	-54.9	-80.5	-78.8	-70.2	-68.4	-66.7	-60.8	-37.7	-17.4

FIGURE A-4. (CONTINUED).

FREE-SPACE SPL FOR HARMONIC NO. 3

VISUAL DISTANCE

PHI, DEG	20.000	15.000	10.000	7.000	4.000	2.000	0.0	-2.000	-5.000	-10.000
-120.00	88.6	111.6	151.2	170.9	182.3	183.8	181.8	178.3	168.0	132.2
-90.00	95.2	91.8	142.4	166.6	182.1	184.9	182.9	178.9	165.8	122.7
-75.00	93.1	84.6	135.9	163.2	181.7	185.5	183.6	179.2	164.0	115.9
-60.00	90.9	91.6	128.1	158.8	180.9	186.2	184.3	179.4	161.6	108.0
-45.00	92.7	95.7	119.0	153.6	179.6	186.8	185.1	179.6	158.7	100.9
-30.00	93.6	96.8	111.3	148.3	178.2	187.2	185.8	179.7	155.6	94.3
-15.00	92.0	96.4	106.5	144.2	176.8	187.5	186.3	179.7	153.1	89.9
0.0	88.5	94.3	106.1	142.5	176.3	187.6	186.5	179.7	152.2	71.3
15.00	86.3	90.8	107.3	144.1	176.8	187.5	186.3	179.7	153.1	87.9
30.00	87.8	89.2	112.4	148.3	178.2	187.2	185.8	179.7	155.6	95.0
45.00	88.2	90.8	120.2	153.6	179.6	186.8	185.1	179.6	158.7	98.6
60.00	85.3	92.0	128.3	158.8	180.9	186.2	184.3	179.4	161.6	107.1
75.00	77.6	94.1	135.9	163.2	181.7	185.5	183.6	179.2	164.0	116.1
90.00	77.5	98.4	142.4	166.6	182.1	184.9	182.9	178.9	165.8	122.5
150.00	78.7	119.3	155.8	172.9	182.2	183.1	181.1	178.0	169.0	137.4

SPL ON THE FUSELAGE FOR HARMONIC NO. 3

VISUAL DISTANCE

PHI, DEG	20.000	15.000	10.000	7.000	4.000	2.000	0.0	-2.000	-5.000	-10.000
-120.00	75.9	85.5	103.6	123.3	135.7	139.1	140.6	134.2	151.7	127.5
-90.00	86.8	82.6	110.7	135.7	154.1	160.2	162.2	170.0	164.4	124.5
-75.00	87.7	78.3	109.3	138.5	160.8	168.9	174.6	178.4	166.4	120.0
-60.00	85.1	81.0	104.1	138.6	165.8	176.6	183.6	182.6	165.7	113.9
-45.00	75.3	85.2	97.7	136.7	169.0	183.2	188.2	184.2	163.3	107.0
-30.00	79.4	87.0	96.5	133.1	170.3	187.1	190.3	184.5	160.3	97.3
-15.00	86.5	86.7	83.9	128.6	169.6	188.4	191.1	184.5	157.9	93.3
0.0	88.7	84.9	90.3	125.2	167.1	187.1	191.0	184.4	156.9	94.1
15.00	87.9	82.7	88.3	123.2	165.7	185.0	189.6	184.2	157.7	96.7
30.00	84.1	81.3	70.1	122.3	159.9	176.4	185.6	183.0	159.5	99.1
45.00	76.9	80.2	83.3	122.2	155.6	169.1	177.4	179.5	160.5	99.4
60.00	82.2	79.6	88.3	121.3	149.9	160.8	164.6	172.2	159.6	107.3
75.00	85.4	81.4	95.2	117.6	142.4	151.2	154.8	159.7	156.1	111.3
90.00	85.3	83.6	86.6	113.3	133.6	140.4	143.5	134.9	150.1	111.1
150.00	71.7	76.9	93.5	97.6	98.5	109.8	100.3	110.4	115.3	100.3

BOUNDARY LAYER AND FUSELAGE REFLECTION DB CORRECTION FOR HARMONIC NO. 3

VISUAL DISTANCE

PHI, DEG	20.000	15.000	10.000	7.000	4.000	2.000	0.0	-2.000	-5.000	-10.000
-120.00	-12.7	-26.1	-47.6	-47.6	-46.6	-44.7	-41.2	-44.1	-16.3	-4.7
-90.00	-8.3	-9.2	-31.7	-30.9	-28.0	-24.6	-20.6	-8.9	-1.4	1.8
-75.00	-5.3	-6.3	-26.6	-24.7	-20.9	-16.7	-8.9	-0.8	2.4	4.1
-60.00	-5.8	-10.7	-24.0	-20.1	-15.1	-9.6	-0.8	3.2	4.1	5.9
-45.00	-17.3	-10.5	-21.4	-16.9	-10.6	-3.6	3.1	4.6	4.6	6.1
-30.00	-14.2	-9.8	-14.8	-15.2	-7.8	-0.1	4.5	4.8	4.7	3.0
-15.00	-5.5	-9.7	-22.7	-15.6	-7.3	0.9	4.7	4.8	4.7	3.4
0.0	0.2	-9.4	-15.8	-17.4	-9.2	-0.5	4.5	4.8	4.7	22.8
15.00	1.7	-8.1	-19.0	-20.9	-13.2	-4.5	3.3	4.5	4.6	8.7
30.00	-3.8	-8.0	-42.3	-26.0	-18.2	-10.9	-0.2	3.4	3.9	4.2
45.00	-11.3	-10.6	-36.9	-31.4	-24.1	-17.7	-7.8	-0.1	1.9	0.8
60.00	-3.1	-12.5	-40.0	-37.5	-31.0	-25.4	-19.7	-7.2	-2.0	0.3
75.00	7.8	-12.7	-40.8	-45.6	-39.2	-34.3	-28.8	-19.4	-7.9	-4.9
90.00	7.8	-14.8	-55.8	-53.3	-48.5	-44.5	-39.4	-43.9	-15.7	-11.4
150.00	-7.0	-42.4	-62.2	-75.3	-83.7	-73.3	-80.8	-67.6	-53.7	-37.1

FIGURE A-4. (CONCLUDED).

APPENDIX C - LIST OF SYMBOLS

B = number of blades

B_D = chord to diameter ratio

A_n, B_n = unknown coefficients for boundary layer wave

C_n, B_n = unknown coefficients for scattered wave

C_o = ambient speed of sound

E = Br_T^3/π

G_{mn}, Q_{mn} = source wave coefficients, see Eq. 17

$H_n^{(1)}$ = Hankel function

J_n = Bessel function of first kind

k = ω/c_o

k_r = radial wavenumber (Eq. 8)

k_o = chordwise source wavenumber (Eq. 12)

k_x = axial wavenumber (2π divided by wavelength in axial direction)

m = harmonic of blade passing frequency

M = Mach number of boundary layer flow

M_x = flight Mach number

n = Fourier index for ϕ variation

M_r = blade section relative Mach number

p = acoustic pressure

P = radial variation of pressure

P_n = unit solution of boundary layer equation

r, r_1, r_o, r_T, r_f, r_E = radii, see Figure 4

t = time

t_b = thickness to chord ratio

U = background velocity of boundary layer flow

x = axial coordinate, fixed to aircraft, positive in direction of flow

Y_n = Bessel function of second kind

z = radial coordinate in boundary layer, see Equation 20.

z_o = radius ratio on propeller

ϕ, ϕ_1 = angles, see Figure 4

ϕ_s = phase lag due to blade sweep

ρ_o = ambient density

ω = radian frequency

Ω = angular speed of propeller

ψ_v = Fourier transform of chordwise thickness distribution

$()'$ = $\partial/\partial r$

$()^*$ = complex conjugate

NASA
National Aeronautics and Space Administration

Report Documentation Page

1. Report No.	2. Government Accession No.	3. Recipient's Catalog No.
NASA CR 185195		

4. Title and Subtitle	5. Report Date
Unified Aeroacoustics Analysis for High Speed Turboprop Aerodynamics and Noise. Volume V - Propagation of Propeller Tone Noise Through a Fuselage Boundary Layer	May 1991
	6. Performing Organization Code

7. Author(s)	8. Performing Organization Report No.
B. Magliozzi and D. B. Hanson	None
	10. Work Unit No. 535-03-01

9. Performing Organization Name and Address	11. Contract or Grant No.
Hamilton Standard Division United Technologies Corporation PO Box 1000 Windsor Locks, CT 06096	NAS3-23720
	13. Type of Report and Period Covered Contractor Report Final
12. Sponsoring Agency Name and Address National Aeronautics and Space Administration Lewis Research Center Cleveland, Ohio 44135-3191	14. Sponsoring Agency Code

15. Supplementary Notes

Project Manager, Bruce Clark,
Advanced Turboprop Project Office, NASA Lewis Research Center, Cleveland, Ohio 44135

16. Abstract

This report presents a unified theory for aerodynamics and noise of advanced turboprops. Aerodynamic topics include calculation of performance, blade load distribution, and non-uniform wake flow fields. Blade loading can be steady or unsteady due to fixed distortion, counter-rotating wakes, or blade vibration. The aerodynamic theory is based on the pressure potential method and is therefore basically linear. However, non-linear effects associated with finite axial induction and blade vortex flow are included via approximate methods. Acoustic topics include radiation of noise caused by blade thickness, steady loading (including vortex lift), and unsteady loading. Shielding of the fuselage by its boundary layer and the wing are treated in separate analyses that are compatible but not integrated with the aeroacoustic theory for rotating blades. The report is in 5 volumes with titles and contractor report numbers as follows.

Volume I. "Development of Theory for Blade Loading, Wakes, and Noise", (CR 4329)
Volume II. "Development of Theory for Wing Shielding", (CR 185192)
Volume III. "Application of Theory for Blade Loading, Wakes, Noise, and Wing Shielding", (CR 185193)
Volume IV. "Computer User's Manual for UAAP Turboprop Aeroacoustic Code" (CR 185194)
Volume V. "Propagation of Propeller Tone Noise Through a Fuselage Boundary Layer", (CR 185195)

17. Key Words (Suggested by Author(s))	18. Distribution Statement
Prop-Fan, High Speed Turboprop, Aerodynamics, Noise, Acoustic Shielding, Vortex Lift, Unsteady Lift, Wakes	General release

19. Security Classif. (of this report)	20. Security Classif. (of this page)	21. No of pages	22. Price*
Unclassified	Unclassified	67	

*For sale by the National Technical Information Service, Springfield, Virginia 22161

NASA-Langley, 1990